Delft University of Technology
Master's Thesis in Embedded Systems

Using Static Objects for Passive Communication with Sunlight

Chaitra Pai

embedded software

TU Delft Delft University of Technology

Using Static Objects for Passive Communication with Sunlight

Master's Thesis in Embedded Systems

Embedded Software Section
Faculty of Electrical Engineering, Mathematics and Computer Science
Delft University of Technology
Building 28, Van Mourik Broekmanweg 6, 2628 XE, Delft, The Netherlands.

Chaitra Pai
c.j.pai@student.tudelft.nl

24^{th} August 2018

Author
Chaitra Pai (c.j.pai@student.tudelft.nl)

Title
Using Static Objects for Passive Communication with Sunlight

MSc presentation
30^{th} August 2018

Graduation Committee

Prof. Dr. K.G. Langendoen (chair)	Delft University of Technology
Dr. M.A. Zúñiga	Delft University of Technology
Dr. Aurèle Adam	Delft University of Technology

Abstract

The idea of having a smart environment to automate day to day tasks appeals to us all. To enable this, we need objects with embedded electronics to communicate with each other in a network known as the Internet of Things (IoT). The IoT communication infrastructure is built on top of existing Radio Frequency (RF) technologies such as Bluetooth Low Energy (BLE), WiFi, and cellular protocols. The RF technology is bandlimited and power hungry, making it unfeasible to support the growing demand of IoT networks. The number of IoT devices in the year 2020 is expected to be around 20 billion, making it essential to explore other areas of sustainable communication technology.

Visible light communication (VLC) in the optical domain is being explored to meet the surge in connected devices and to enable sustainability in the energy consumed. The idea behind a VLC system is to toggle a Light Emitting Diode (LED) at high speed to transmit information which ensures that users are not subjected to visual interruptions. Even sunlight - the biggest source of illumination - can be used to transmit information. However, it is not possible to toggle the sun like LEDs. Hence, the objective of this thesis is to use sunlight to setup a green communication channel.

In the 1800s, sunlight was used to communicate over long distances by using mirrors to reflect light to send signals. Taking inspiration from this method, I propose using smart materials to toggle sunlight and use it for wireless communication. My aim in this thesis is to analyze the behavior of smart materials, develop a modulation scheme suitable to send information using sunlight, and evaluate the system's performance.

Preface

This report is the consolidation of my Master of Science thesis with the Embedded Software group over a period of 10 months. My journey in exploring optical communication started in June 2017 at my summer internship, where I got introduced to the idea of Visible Light Communication (VLC).

I was working on a navigation project that used LEDs to localize people in an indoor environment. I got an opportunity to understand how the ubiquity of lights can be used to develop an efficient indoor localization platform. My interest in VLC developed then and I approached Marco Zúñiga to discuss the possibility of a thesis in this area. Sustainable communication using sunlight was of my interest; thus, I decided to pursue my MSc thesis in designing a system to enable this communication. To fulfill this objective, static surfaces need to be analyzed to work as a transmitter and is the primary focus of my thesis.

I would like to express my gratitude to everyone who has been instrumental in the successful completion of my thesis. Firstly, I would like to thank my supervisor Marco for his guidance, support and motivation throughout my thesis. I would like to thank Rens for sharing his knowledge on the topic and providing valuable inputs during this time. I would also like to thank Eric and Ioannis for their constructive insights on my thesis.

I would like to thank all the MSc students in the VLC group for providing valuable feedback during the group meetings. Lastly, I would like to thank my parents, friends and my extended family for being the pillar of strength and support during this period. Their love and motivation has been the driving force for the successful completion of my thesis.

Chaitra J Pai

Delft, The Netherlands
24th August 2018

Contents

Chapter 1

Introduction

Society was formed due to the dependency between men to avail the basic necessities of life; thus, communication came into existence. Gestures were the earliest form of communication used by man to convey his thoughts and feelings to the people in his surroundings. Over time, the need for long distance communication rose as they wanted to warn the people around about potential threats lurking them. Smoke signals were an easy an effective solution to do so. The need to convey information began man's journey into exploring different communication methods.

The earliest forms of communication also included drums, honing pigeons etc. before we moved into electrical communication systems such as telegraphs in the 1800's. We then evolved into better techniques such as Morse codes (1837), telephones (1876), radio (1894), satellite communication (1958) etc., leading to the rapid growth of the communication sector; making people across the globe feel connected and up to date. The radio frequency (RF) spectrum was harnessed to its fullest to enable these technological advances.

The extensive use of RF for communication made it a victim of its own success. The incessant use has resulted in extreme saturation of these channels, that has led to a substantial amount of energy consumption. This gives rise to a very important question - Can a different region of the electromagnetic spectrum be used to enable eco-friendly communication? The motivation behind this thesis is to revive the oldest and potentially the greenest form of energy for communication - sunlight.

1.1 History of sunlight based communication

The idea of using energy from the sun to communicate information exists from centuries. However, nowadays, the energy from the sun is harvested to generate a non polluting and a sustainable alternative to fossil fuels. There are two prominent technologies from the yesteryears that successfully used the sun that is 149.6 million km away from earth for communication.

1.1.1 Heliograph

The Heliograph was developed in the 19^{th} century to transmit signals, enabling long distance communication. It is a form of wireless communication where a mirror is used to reflect sunlight from its surface. The mirror is pivoted or blocked with a shutter to send flashes of coded information (Morse code) as shown in Figure 1.1. The size of the mirror, the direction of pointing it to the right location, and the weather conditions determine the communication range of the heliograph. A range of 48 km is observed under normal lighting conditions. Militaries around the globe used this technology to send signals across terrains in the late 19^{th} and early 20^{th} centuries [26].

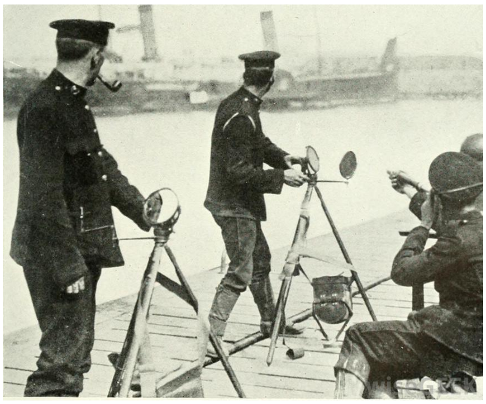

Figure 1.1: Heliograph being used by the military at the docks [16].

1.1.2 Photophone

Another piece of technology that worked using sunlight was the photophone, discovered by Alexander Graham Bell in the 1880s. Telephones send voice over electric wires whereas photophones use sunlight for the same. Sunlight is angled at the mirror placed in front of the microphone on the transmitter side. The vibrations caused by the voice signals move the mirror back and forth, modulating the light that was incident on the mirror. The receiver comprises of a selenium photoelectric sensor that converts the light signals back to voltage and the headphones receive the sent audio message as shown in Figure 1.2.

The communication range of 213 meters was achieved with the photophone in the presence of sunlight [27]. It was one of the first successful attempts to a wireless voice transmission system. Graham Bell said about the photophone - "the greatest invention [I have] ever made, greater than the telephone", indicating that the principles behind this design are noteworthy and can be explored further.

These early technological advances are the inspiration for my thesis focusing on the use of sunlight. The novelty in my thesis is the usage of smart materials which can vary their transparency levels, leading to advancement in the field of optical communication.

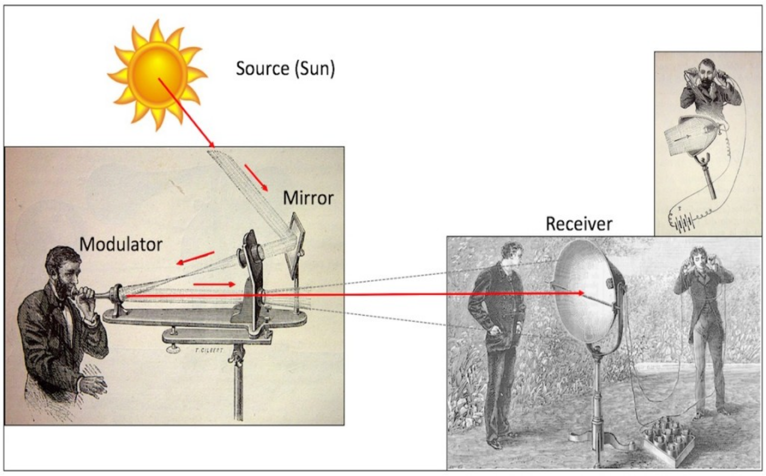

Figure 1.2: Illustration of the working of a photophone [7].

1.2 Problem statement

The objective of this thesis is to set up a communication system (physical layer) using the visible light region of the electromagnetic spectrum. The system will not use conventional light sources such as LED lamps but, will use sunlight instead. The sun, being an uncontrollable source of light needs the support of additional hardware (e.g. smart materials that can change light intensities) to function as a transmitter in a communication system.

The three main goals of the thesis are:

1. Analysis of smart materials: There are materials that have the potential to change the intensity of the light. They are being used for applications where you need to limit the amount of light entering a space (e.g. airplane windows, smart glasses in offices etc.). In this thesis, these materials are analyzed for their ability to modulate sunlight for communication.

2. Modulating sunlight: The challenges that occur while modulating sunlight are quite different when compared to modulating radio waves or LEDs. A modulation scheme, suitable to most of the off-shelf smart materials is developed.

3. System evaluation: The novel communication system designed is evaluated for essential parameters such as: data rate, communication range, and power consumption.

1.3 Contributions

Sunlight based communication using modern day hardware has been an unexplored territory. The appropriate use of the hardware to function as a transmitter needs to be investigated along with suitable data transmission techniques. The contributions of the thesis within this context are:

- Design and development of the physical layer of the communication channel using static objects. This is done by analyzing the properties of the smart materials.
- Implementation of a modulation scheme that harnesses the smart material properties to design a flicker free and stable transmission system.
- Evaluation of the performance parameters of the system.

1.4 Application of the proposed system

One of the key features of this system is the use of sunlight to modulate information. The physical layer designed in this thesis will act as a foundation to the development of a sunlight based communication system.

Figure 1.3: Communication using smart materials.

Let us consider a scenario where a tourist visiting Delft needs to download a map of the city. He does not have a data plan or public WiFi at his disposal. When he comes close to a tram stop, he is able to successfully download the map and find his way through the city. The communication between his phone and the surface of the tram stop is made possible by the smart materials installed on the surface of the tram stop. These materials are able to modulate the sunlight and send signals to the phone as shown in Figure 1.3. The surface is also capable of sending information to multiple users in the vicinity, providing a green communication alternative. The work done in this thesis will contribute towards achieving this objective.

1.5 Report format

Chapter 2 provides background information on VLC and gives an overview of the prior research work done that is relevant to the thesis. The transmitter and receiver design is discussed in Chapter 3. The smart materials under test to work as transmitters are analyzed for their behavioral traits in Chapter 4. Chapter 5 discusses the pros and cons of the modulation schemes that are suitable to the material behavior. The performance parameters of the system are measured in Chapter 6. The conclusion of this thesis along with the possible future work is discussed in Chapter 7.

Chapter 2

Background and related work

This chapter provides background information on Visible Light Communication (VLC). Section 2.1 gives information on the types of communication enabled by regions in the electromagnetic spectrum. The channel characteristics while using sunlight to communicate are discussed in 2.2. Section 2.3 sheds light on the research goals of this thesis. The relevant work done on VLC in the past decade is discussed in 2.4.

2.1 Electromagnetic spectrum - Visible light

The electromagnetic (EM) spectrum is comprised of different classes. Each class is categorized based on the frequency range into microwaves, radio waves, x-ray etc as shown in Figure 2.1 [25] .

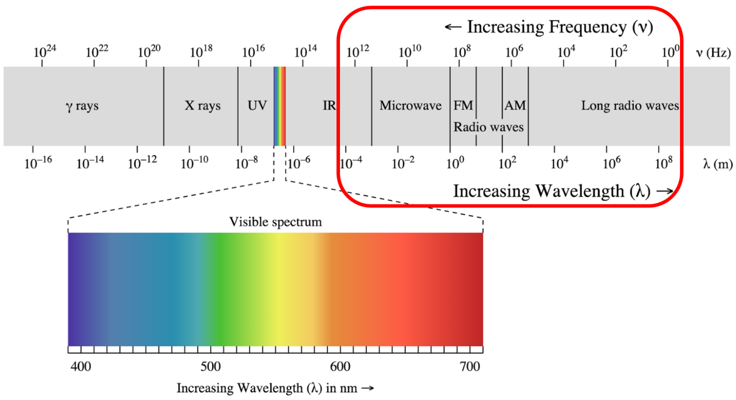

Figure 2.1: Electromagnetic spectrum composition [12].

Out of these classes, radio waves are widely used for communication with the spectrum ranging from 3Hz to 3Thz as highlighted in Figure 2.1. The number of users using radio spectrum surged in the last few decades because of the rapid growth in cellular communication and connected devices (Internet of things). This resulted in the development of alternative approaches such as frequency reuse and cognitive radio [28].

Researchers started to investigate on the use of other classes of the EM spectrum which can support communication. The visible light region is one such space which can be used and has a spectrum ranging from 430 THz to 770 THz. To setup a communication system using visible light, we have two categories of light sources-

1. Artificial light- This type of light source includes LED lamps, fluorescent bulbs etc. which can be controlled to act as a transmitter. They are ubiquitously found in indoor and outdoor environments making it a very convenient emission source.

2. Natural light- Sun, being a primary source of illumination on earth, is a major transmission source in this category. The work done in this thesis is going to focus on using sunlight (ambient light) as the primary light source of the VLC system.

2.2 VLC with sunlight

The pre-requisite of any communication system is the ability to change a signal (i.e. modulate) to enable data transmission. In case of light based communication, this is made possible by toggling LEDs at high frequencies to change the intensity of light to transmit data. The high frequencies of switching ensure that the flickering of light is not observable to the human eye. The modulation in artificial light sources is brought about by attaching an external driver circuit and implementing some software changes. It is obvious the such control cannot be established while using sunlight. Thus, there are different types of communication channels to cater to the variations in the light source.

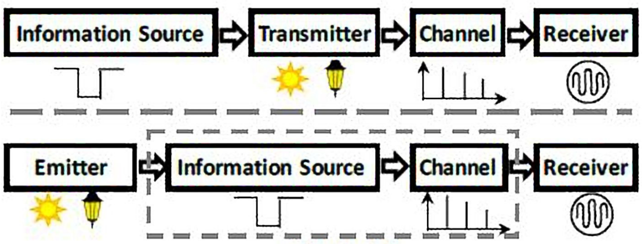

Figure 2.2: Communication channel standard (above) and passive (below) [23] .

Active communication channel

The traditional communication channel that is used comprises of the information source, transmitter, channel and receiver as shown in the upper part of Figure 2.2. The information source is the data which is represented in a binary format while the transmitter is a source like LED which sends this binary data. The channel refers to the environment in which the signal (i.e. light) propagates and the receiver here is a photosensitive sensor that captures the light signals.

Passive communication channel

The above explained channel is not suited for communication using sunlight as the transmitter is uncontrollable. The communication channel is modified by swapping the positions of the emitter (transmitter) and the information source as shown in the lower part of Figure 2.2. This implies that there is a need for the information source to be self sufficient i.e. to decide what signal it needs to send by modulating the light source.

An implementation of communication using such a channel is explained in [6], [23]. The setup for this system is shown in Figure 2.3. A barcode is placed on top of the car (or on the doors) and does not consume any energy on its own. The receiver is placed on a pole under which the car passes by (or on the side of the road if barcode is placed on the door). When the car passes below (in front of) the receiver, light is reflected from

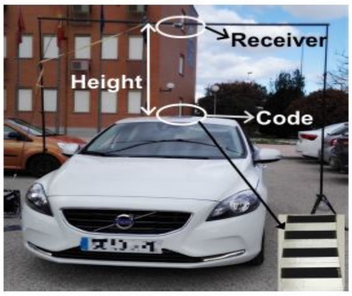

Figure 2.3: Setup of a barcode based passive communication channel [23] .

the barcode surface. The movement of the car is able to vary the intensity of the reflected light as the barcode changes color below (in front of) the receiver from white to black or vice versa. This generates a modulated signal which is then decoded at the receiver as shown in Figure 2.4. This setup can be referred to mobile object communication with barcodes.

If in the above setup, the car is stationary, the receiver will capture the reflected light from the barcode and we will not be able to see any variations in the signal. This is because the movement of the car was instrumental in

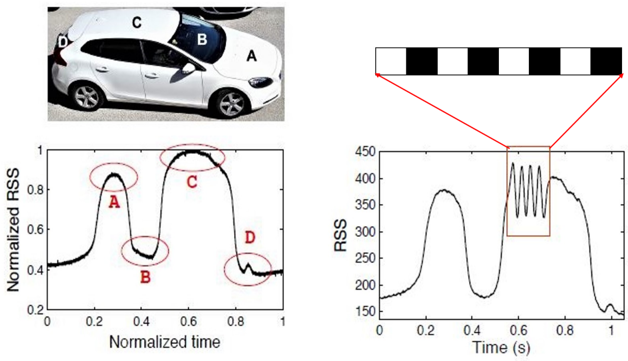

Figure 2.4: Shape of the car detected by the receiver (left) and the variations of the barcode captured when placed on the roof of the car (right) [23] .

changing the position of the black and white stripes that came in view of the receiver. It can also be termed as static object communication due to the immobility of the barcode. The major challenge in this case is to enable signal modulation when objects are stationary. The thesis does address this challenge and focuses on enabling passive visible light communication using static objects. Figure 2.5 gives an overview of the above discussed methods, highlighting the novelty of this thesis.

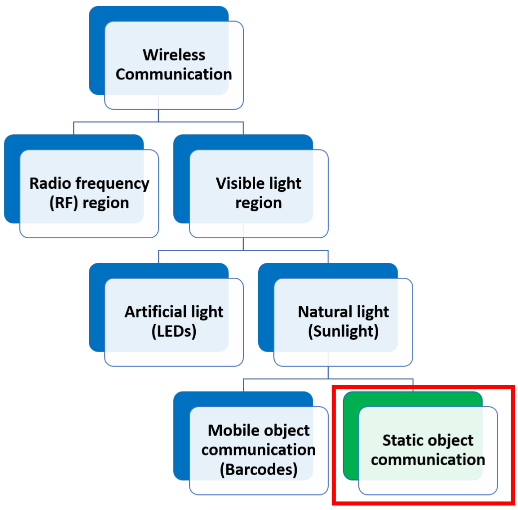

Figure 2.5: Wireless communication methods; focus of this thesis is on static object communication.

2.3 Research goals

The main objective of the thesis is to design the physical layer of the communication channel where we can use static objects to modulate information using ambient light. The research goals are to:

1. Analyze the behavior of off the shelf smart materials and design a transmitter which can be toggled to send information using sunlight.

2. Design a modulation scheme that complements the material behavior and enables transmission with minimal perceivable flickering.

3. Decode the received signals using a suitable algorithm. Measure the system parameters such as the data rate, power consumption and communication range.

2.4 Related work

The pioneering research done by Bell in the field of light communication in 1880 was not further researched until the last decade, where researchers started to investigate the communication using visible light. Some of the notable contributions done in this area that have drawn inspiration to the thesis are discussed in this part.

2.4.1 Traditional approach to VLC - Active communication

VLC using artificial lights found applications in many fields, and indoor navigation and localization is one among them. The pervasiveness of artificial lighting in indoor spaces draws attention to this application.

VLC with LEDs and light sensors

The indoor navigation platform in [9] aims to enable a energy efficient alternative to GPS with lights. The existing lighting infrastructure with additional hardware (microncontroller and switching circuit) is used to control the toggling of LEDs for data transmission. This setup forms the transmitter which transmits a unique identification (UID) code that is pre-defined based on the LED position indoors, The receiver is a custom design with a light sensor to detect the signal changes, filtering circuits to remove high frequency noise components and a microcontroller to decode the received UID signals and indicate the user position on the screen. There is a keyboard at the receiver end which is used to enter the destination address. The data transmission rate of the LED is 2 kbps for a 18 bit UID data frame with a communication distance of 1.8m.

VLC with LEDs, smartphone, and light sensors

VLC based navigation for the visually impaired works on a similar concept but with the addition of a smartphone and headset at the receiver [17]. The user activates the indoor navigator and give a voice input of his destination. The route information is accessed from the cloud service using WiFi and when the user is in motion, the receiver captures the light signals from above and sends it via Bluetooth to the smartphone for processing.

An additional aid to this system is provided by the orientation of the smartphone indicated by the value received from the geomagnetic sensor. The UID of the LED is mapped to its location co-ordinate (from the cloud service) to compute the direction; paired with the orientation to guide the user to the destination using audio signals. The system has a data rate of 4.8 kbps and a frame size of 128 bits with a position accuracy of 1-2m. The major drawback of this system is that there are multiple communication protocols used (WiFi, Bluetooth and VLC), making it a power hungry system.

VLC with a smartphone camera

A different approach to implementing indoor positioning is done just by using off the shelf smartphones without any additional paraphernalia [13]. The setup is similar to the previous case, excepting the use of audio signals and a sensor based receiver. The idea here is to process the information using the Complementary Metal Oxide Semiconductor (CMOS) cameras on the smartphones. The camera captures images in which the LED lights are detected and the user location is processed using a cloud server.

The frame rate of camera is 30 frames per second (fps) which is very low compared to the data transmission rate of LEDs (usually in kHz). To enable capturing the high frequency signals from the LEDs, the rolling shutter effect of the camera is used. The light signals incident on the CMOS pixels are converted to their equivalent voltage which represents as pixel value. These pixels are placed sequentially and the CMOS sensor is exposed line by line which enables to detect the fast changing LED signals effectively [8]. The communication range for this setup is 1m with a data transmission rate of 1 kbps.

VLC for sensing

VLC also finds application in areas where illumination control is needed [10]. The lighting levels in an indoor environment are determined based on occupants in the room. Luminaires are equipped with occupancy sensors which monitor the number of people in the room. At a given instance of time, a single luminaire is communicating with the rest by modulating its light intensity; which is then captured by the light sensors on the other luminaires. A centralized controller processes this information and determines the dimming levels that need to be established in the space thereby enabling a stable and energy efficient lighting control.

2.4.2 VLC - Semi-passive communication

In semi-passive communication, the downlink transmission is based on the concept of traditional VLC whereas, the uplink data transmission is based on the reflection of light with smart materials.

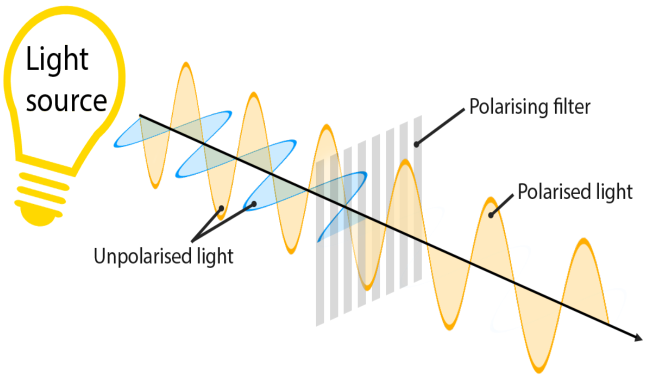

Figure 2.6: Polarization of light [5].

One method to generate uplink signals is by varying light intensities using polarizers. Light is a transverse, electromagnetic wave which has vibrations in multiple planes. This multi-planar vibrating light waves are termed as unpolarized light. Polarizers are materials which blocks light in all planes of vibration except the one parallel to its polarization axis as shown in Figure 2.6. This is the same material used in sunglasses to reduce the glare from sunlight.

Two polarizers are placed with their polarization axes parallel to one another as shown on the right on Figure 2.7. The unpolarized light is polarized parallel to the axis of the first polarizer which is then emitted as light from the other polarizer (aka analyzer). When the polarizers are placed with their axes orthogonal to one another, there is no light at the analyzer as shown on the left of Figure 2.7. The light intensity can be mechanically controlled by using polarizers and we can enable light based data transmission. The materials used in the uplink of the semi passive communication achieve a similar output but, in a well synchronized and controlled manner.

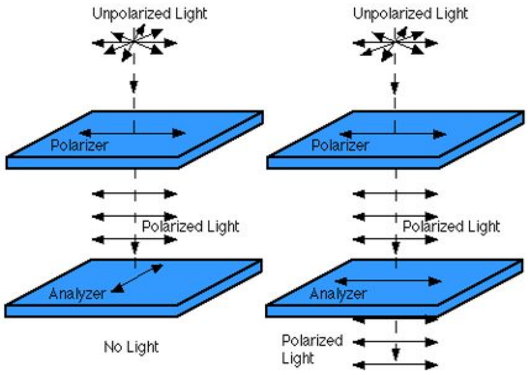

Figure 2.7: Output of the polarizer- no light exiting analyzer (left) and polarized light exiting analyzer (right) [15].

Retro VLC

Retro VLC aims at setting up a bidirectional communication platform [14]. The downlink (ViReader) has an LED (controlled using a driver circuit) and a photodiode to capture the light changes. The uplink (ViTag) comprises of a solar panel, photodiode, LCD shutter (smart material) and a retro-reflective material as shown in Figure 2.8.

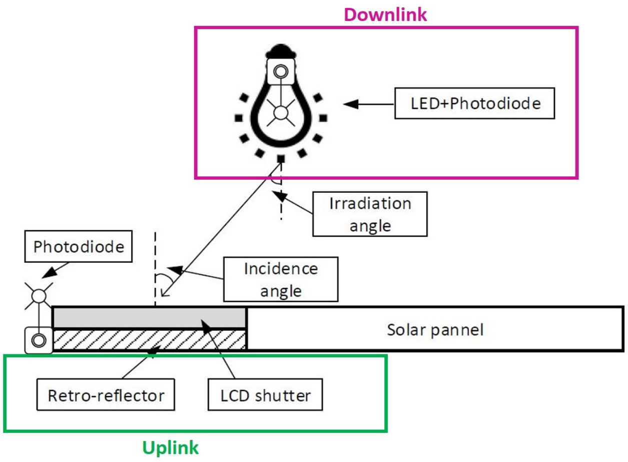

Figure 2.8: Bidirectional visible light communication with backscattered light [14].

The downlink communication works similar to a traditional VLC system whereas, the uplink is based on the light modulation by the smart material. The retroreflective material (like the stripes on safety jackets) ensures that the light from the ViReader is reflected back to the photodiode near the LED but, the data transmission is controlled by the smart material. Here, the uplink is totally dependent on the downlink for transmission. The work done in my thesis does not have any downlink dependency, making it novel when compared to this system. The data trasnmission rate for the downlink and uplink are 1 kbps and 0.5 kbps respectively with a maximum communication distance of 2.4m.

Passive VLC

Passive VLC [29] is an upgraded version on Retro VLC discussed above. The objective here is to enable faster uplink data transmission by implementing hardware and software modifications.

The smart material has a maximum switching frequency based on the supply voltage. If the material toggles any faster, the probability of distinguishing the signals reduces and we face detection error. Passive VLC implements this fast toggling system and enables successful decoding by splitting the received signals into smaller segments and comparing them to a reference signal. This enables to decode signals effectively and also have a data transmission rate of 1 kbps on the uplink.

Indoor positioning with visible light (PIXEL)

PIXEL is a VLC based indoor positioning technology [30] that eliminates the need of accurate alignment between the transmitter and the receiver. The transmitter consists of an LED lamp, modified LCD pixel (discussed in Chapter 3) and a optical rotatory material (dispersor) that splits white light into its constituent colors as shown in Figure 2.9. The receiver is a smart phone which has a polarizer attached on its camera.

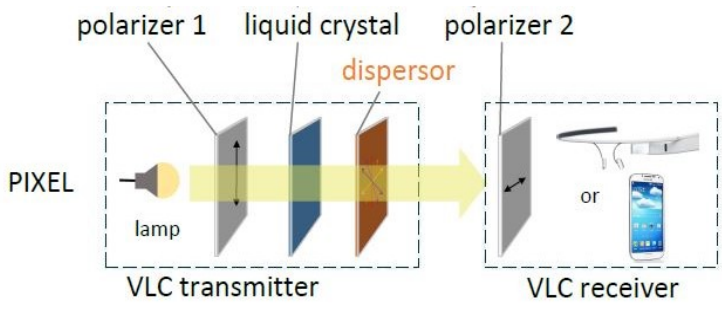

Figure 2.9: Indoor positioning system using color based light modulation [30].

Unidirectional modulated light at the transmitter is split into its constituent colors by the dispersor. On the other hand, the smartphone camera visualizes the color which is let in by the polarizer at a given orientation.

The colors for each bit (0/1 in this case) will be distinct for any orientation of the receiver, improving the flexibility in localization with VLC. The data transmission rate for this system is 14 Hz with a communication distance of 10m at a video resolution of 120X160 pixels.

Method	**Data Rate (kbps)**	**Communication range (m)**
VLC with LED and light sensors	2	1.8
VLC with LED, light sensor and smartphone	4.8	1-2
VLC using CMOS camera	1	1
Retro VLC	0.5	2.4
Passive VLC	1	3.3
PIXEL	0.014	10

Table 2.1: Data rate and communication range achieved for the methods discussed above.

Table 2.1 gives an overview of the above discussed VLC implementations based on their data rates and the communication range . There is a clear trade off observed between improving the data rate and the communication range. In case of PIXEL, the range is almost 5 times that of the other implementations with a data rate of 14 bps. The ideation of this thesis is based on the use of similar materials but, differs from state of the art by using sunlight to communicate and is discussed in the next chapters.

Chapter 3

System design - The physical layer

This chapter mainly focuses on the physical layer design for the communication system. The design requirements are discussed in Section 3.1. Section 3.2 provides information on the working of the smart material that will be a part of the transmitter design. The hardware and software details of the transmitter are also discussed in this section. A brief explanation on the receiver used for signal capture is done in section 3.3.

3.1 System overview

The system is made up of the transmitter and the receiver; both of which have pre-defined design requirements. The data transmission should be done using sunlight. To enable this, the transmitter needs to be designed using smart materials as modulating sources. On the other hand, the receiver should have a photosensitive component to measure the signal changes. These changes are reflected in the form of varying light intensities whose values need to be digitized using suitable circuitry. The exposure area of the photosensitive material should be limited to avoid interference from the surroundings. These requirements are accounted for and the system is designed as discussed in the coming sections.

3.2 Transmitter

Section 2.5 gives insights on how light can be controlled by varying the orientation of the polarizers. We can vary the intensity of light without any manual control by using materials known as liquid crystal (LC) shutters.

Liquid crystal shutter - Material composition

The innermost layer of the shutter comprises of a liquid crystal layer. Liquid crystal (LC) is a state of matter where the molecules are crystalline in nature and the flow is like that of a liquid. The liquid crystal used in the material is of the twisted nematic (TN) type. This means that the molecules are anisotropic in nature i.e. rod shaped and are oriented in the direction of the long axis as shown in Figure 3.1. LC in the nematic phase can be aligned by application of external magnetic or electric field.

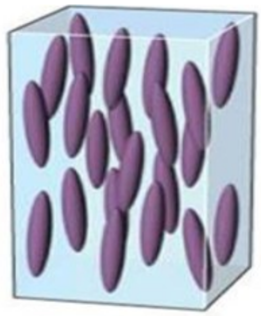

Figure 3.1: Nematic liquid crystal molecules - parallel along the longer axis [3].

This liquid crystal is sandwiched between two glass substrates that are made of borosilicate (no alkali ions) or the ones coated with silicon dioxide as shown in Figure 3.2. This is done to avoid the atmospheric moisture change the orientation of the crystal. Each glass substrate is coated with electrodes facing the LC molecules. Lastly, the glass substrates are externally covered with polarizer films whose axes are orthogonal to each other.

Working of the liquid crystal shutter

The material by default is in a translucent state, that is the electrically off state, where the liquid crystals are helically rotated 90° by the alignment layer (not shown in the figure) coated on the electrodes. Thus, the polarized light passing through the crystal is rotated orthogonal to its initial position by the LC molecules. Thus, the light exits the analyzer as shown on the left of Figure 3.2. When electric field is applied between the electrodes, the helical structure of the crystal is realigned parallel to that of the electric field. This means that the polarized light from the front polarizer is blocked by the liquid crystal; making it perpendicular to the rear polarizer axis. This results in no light being emitted from the rear polarizer as shown on the right of Figure 3.2. The electric torque is responsible for the parallel alignment of the molecules while the elastic torque gets it back to the helical structure.

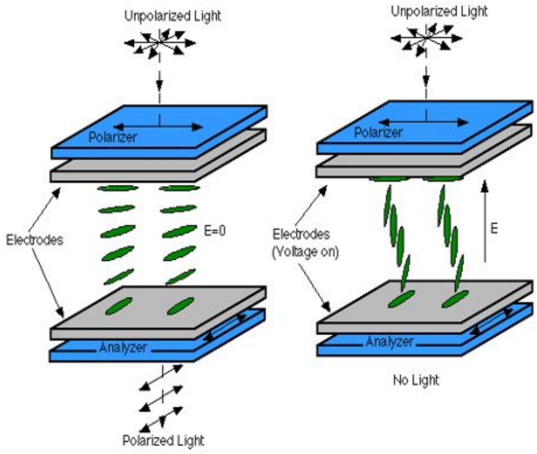

Figure 3.2: Output states of the liquid crystal (LC) shutter- translucent (left) and opaque (right) [15].

The opaqueness of the shutter is determined by the applied absolute voltage. When the voltage increases, the translucency level decreases and vice versa. The experiments are conducted using commercial off the shelf LC shutters that provide no information about the material properties other than the supply voltage. The speed at which the switching occurs is primarily dependent on how efficiently the crystals can be steered in the medium. Is it also dependent on the cell gap which is the gap created between electrodes by filling the liquid crystal; smaller cell gap resulting in faster switching. Thus, the maximum switching speed of the LC shutter is dependent on the manufacturer design, making it a major limitation of using these materials. The requirements of high switching speeds can be easily satisfied by using customized high speed shutters, and are not very cost efficient. Thus,the experiments are conducted on off-shelf LC shutters to have a cost-efficient and easy to manufacture transmitter.

3.2.1 Intensity based modulation

The modulation is implemented on the LC shutter by voltage changes; resulting in light signals of varying intensity. The receiver is able to detect these changes and generate a waveform. Hence, the process is termed as intensity based modulation.

The change in the translucency and opaqueness of the LC shutter is visible to the human eye when the switching occurs at slow speed; known as the flickering effect. Prolonged flickering can lead to health issues such as dizziness, headaches, and in extreme cases cause epileptic seizures [4]. According to the VLC standards [19], the maximum frequency time period (MFTP) at which human eye cannot perceive the change in the light intensity (flickering) occurs at 5 ms or less (i.e. minimum frequency higher than 200 Hz).

There is no information provided by the manufacturers on the maximum frequency of the off-shelf LC shutters used in this thesis. Thus, it is essential to perform a thorough analysis on the material behavior as shown in Chapter 4. This will work as a reference baseline for the system design of a specific flicker free application with these LC shutters.

3.2.2 Hardware and software

The transmitter comprises of three parts- the microcontroller(STM32-F446 RE), the driver circuit and the liquid crystal shutter as shown in Figure 3.3(a). The data is modulated and converted into its binary form, ready for transmission at the microcontroller. The microcontroller is configured and programmed using STM32CubeMX software and Keil μvision IDE respectively. The maximum pin output voltage for the microcontroller ranges from 1.7V - 3.6V, and is insufficient to power the shutters as per their voltage recommendations shown in 3.1. The output voltage is boosted using additional driving circuitry which in turn will enable switching the shutter in an efficient manner. A customized driving circuit is designed with an operational amplifier (OPAMP) to drive the shutter at higher voltages with faster switching speeds. LM324AN, with microsecond switching time is used as a non-inverting OPAMP to drive the shutters as shown in Figure 3.3(b).

The liquid crystal shutters used for transmission are of 3 different types with hardware specifications as shown in Table 3.1 [2] [1]. All the shutters are of TN type and are transmissive in nature i.e. they need a light source behind one of the polarizers to modulate its intensity. The shutters are tested for their suitability as a transmitter based on their inherent behavior and performance.

Material name	**Supplier**	**Dimensions**	**Area (in cm^2)**	**Supply voltage**
Rectangular shutter	Adafruit industries	96.5 mm X 38 mm	36.67	5V
Circular shutter	Liquid Crystal Technologies	110 mm diameter	95.03	3V - 15V
Video shutter	Liquid Crystal Technologies	34 mm X 43 mm	14.62	10V +

Table 3.1: Shutter specifications.

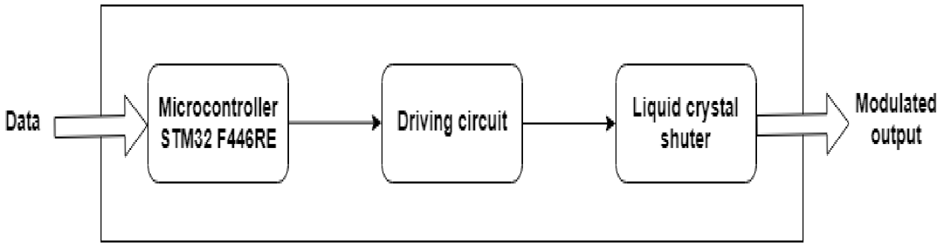

(a) Block diagram of the transmitter

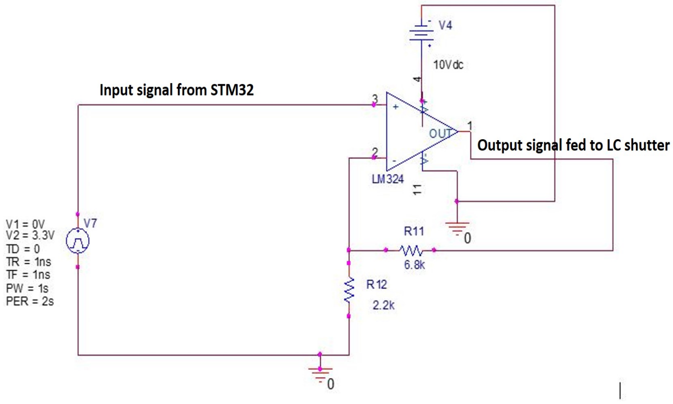

(b) Driving circuit

Figure 3.3: Transmitter design.

3.3 Receiver

The design and analysis of the receiver is done by Rens Bloom, largely in his MSc thesis titled 'Channel analysis for passive communication with ambient light' [6]. The signal from the transmitter is directed to the receiver, which captures the variation in the light intensity using a phototransistor (PT480 by Sharp microelectronics). The receiver processes the light signals as shown in Figure 3.4. The captured light signal from the phototransistor is amplified, and is then fed to the ADC (analog to digital converter - MCP 3201 by Microchip) connected to BeagleBone black. These light signals are then digitized in a format suitable for decoding and further processing. The entire circuit is battery operated to minimize the effects of electromagnetic noise.

This setup is enclosed in a black box made of legos to limit the exposure i.e. the Field of View (FoV) of the phototransistor to external light sources and avoid signal saturation. The receiver is used in this thesis to capture the light signals from the LC shutter to analyze its behavior. The receiver

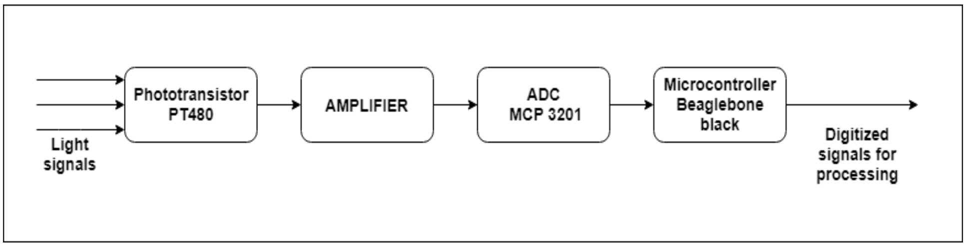

Figure 3.4: Block diagram depicting the structure of the receiver.

samples the signals at 50 kHz. This system is used to perform material analysis and gain insights on its behavior. This will then help determine the type of modulation scheme that can be implemented on the LC shutter. Lastly, the performance parameters of the system are measured and are discussed in the upcoming chapters.

Chapter 4

Material analysis

This chapter focuses on the analysis of the LC shutters used as a transmitter. The experimental setup for the tests performed is explained in Section 4.1. Section 4.2 discusses the output signal behavior. The influence of the voltage on the behavior of the shutter is discussed in Section 4.3 and 4.4 respectively.

4.1 Experimental setup

The smart materials (LC shutters) used in this thesis are not primarily designed for communication (data transmission). Thus, it is essential to analyze the shutters for their performance parameters. To test them, experiments need to be performed in a controlled environment. The results of the analysis will give us a comprehensive idea of the LC shutter performance as a wireless transmitter.

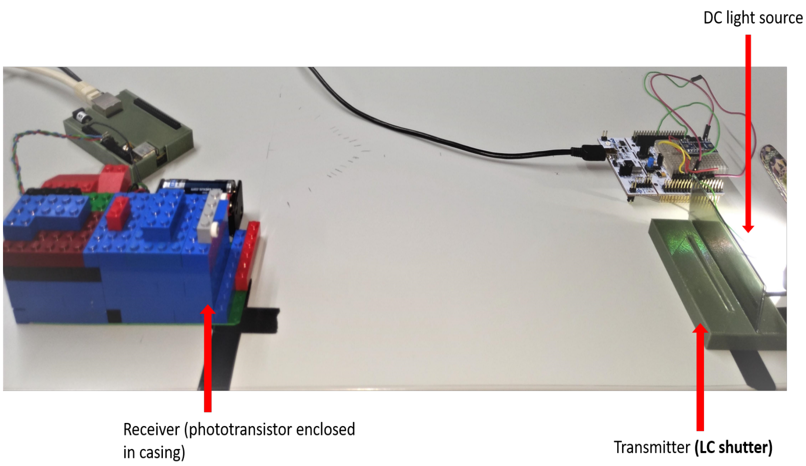

Figure 4.1: Experimental setup with the transmitter (right) and the receiver (left).

The first step towards this objective is to analyze the material for its maximum switching speed. For this, the experiment is performed in a dark room with the transmitter and receiver placed at a distance of 30cm. There is a direct line of sight between the transmitter and the receiver as shown in Figure 4.1. The DC light source is place right behind the transmitter at a distance of about 5-7cm from the shutters. The distance is chosen to avoid the signal saturation at the receiver.

The DC light source, without the presence of a transmitter provides illumination of about 390-400 lux. This is measured with a lux meter placed at the same position as the receiver. The receiver is enclosed in a lego casing and has an opening of 10 mm X 16 mm. The size of the opening determines the amount of light that can be captured at the receiver. The shutter is toggled (switched on/off) to generate signals, which is then captured at the receiver with a sampling frequency of 50 kHz and signal analysis is performed.

4.2 Input output characteristics

The amount of light that passes through the LC shutter is controlled by the voltage supplied to it. In other words, the voltage controls the opacity of the shutters under test. The objective here is to understand the variation in the opacity of the shutter for different voltage values.

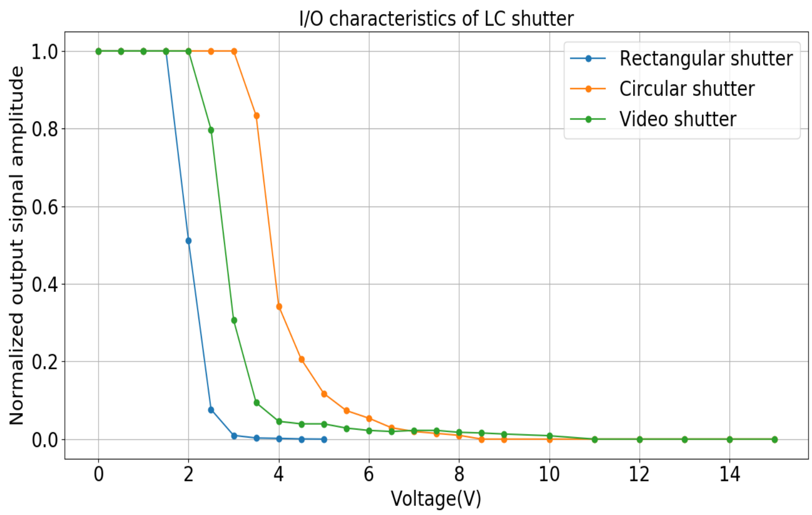

Figure 4.2: Normalized output signal amplitudes for different LC shutters.

Maximum light intensity is received by the phototransistor when there is no voltage supplied to the shutter, as it is translucent by default. As the applied voltage increases, the received light intensity starts decreasing i.e.

the opaqueness of the shutter keeps increasing. For each of the shutters, the output signal intensity for varying (drive) voltage values are measured at the receiver. The normalized output signal values for each of the three shutters are shown in Figure 4.2.

The larger the value of the applied voltage, the higher the signal contrast. The reasoning behind this has to do with the LC molecules. When voltage is applied, the molecules align parallel to the electric field as explained in Section 3.2 and we observe opaqueness. The minimum threshold value needed to begin this alignment is also known as Freedericksz threshold voltage (V_{th}). The realignment continues until the saturation voltage (V_{sat}) is reached, at which maximum alignment of the molecules to the electric field occurs [20].

From the graph, the empirical values V_{th} and V_{sat} values for the rectangular, circular, and video shutter are (1.8V, 3V), (3.5V, 8V), (2.3V, 10.5V) respectively. These values indicate the voltage range, which when applied can switch the shutter from the translucent to the opaque state respectively. Thus, we can conclude that, the higher the voltage value, the stronger is the opaqueness. The second observation is that, the amplitude of the signal is same for multiple voltage values. The change in the signal state from translucent to opaque is not observed when toggled between these voltages. This results in the LC shutter exhibiting non linearity (a sharp transition between high and low levels). It also indicates that a single shutter cannot generate modulation signals at varying amplitude levels for all voltage values. Thus, it is difficult for a single LC shutter to use modulation schemes such as PAM (Pulse Amplitude Modulation).

4.3 Response time

The analysis in Section 4.2 clearly indicates that the signal contrast is determined by the applied voltage. The goal here is to compute the maximum data rates which is determined by the maximum operating frequency of each of the three LC shutters. This is computed by measuring the slope of the signal while switching from 0 to 1 and 1 to 0 respectively.

The upper bound for the switching speed of the LC shutter can be determined by measuring the response time. It is an indication of how the shutter responds to high speed signal changes, and is computed as the average of the rise and fall times. The rise time is the amount of time required to switch from the opaque (off) to the translucent (on) state, while the fall time is that needed to switch back to the opaque state. In other words, it is the transition time from the lowest to the highest measured amplitude and contrariwise. The maximum operating frequency is a reciprocal of the average response time which is calculated based on the received signal. The rise and fall times are measured between 10% and 90% of the total signal amplitude, using the setup explained in Section 4.1.

Driving the shutters at 5V

Based on the observations made in 4.2, all the shutters turn opaque when powered with 5V, which is chosen as the supply voltage for this experiment. The microcontroller toggles the shutter at 1 Hz, enabling it to transit between the translucent and opaque states. The values corresponding to this change are captured at the receiver, and are used to compute the response time.

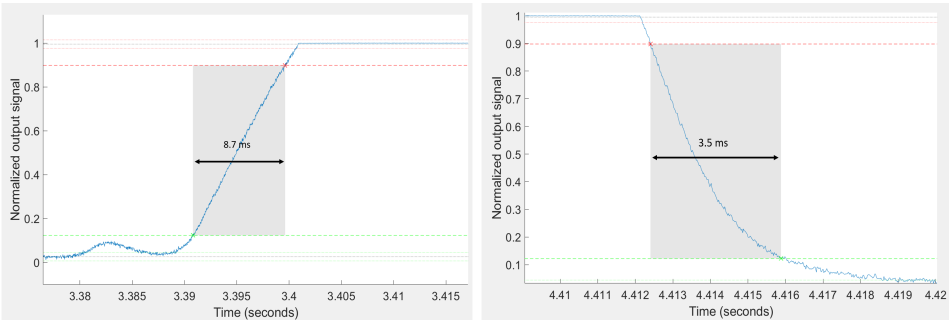

(a) Rise time (b) Fall time

Figure 4.3: Rise and fall times of the rectangular shutter at 5V.

The mechanism of the molecule orientation needs to be understood to analyze the rise and fall time behavior. The molecule alignment either results in a translucent or an opaque state. As stated in Section 3.2, the molecules of the LC are of the twisted nematic type, and have a default resting position (helical) when no voltage is applied. Thus, the default output state is to be translucent. The rise time indicates that the molecules are realigning to the helical orientation when the applied voltage is reduced to 0V. This realignment is performed by the elastic torque on the LC molecules [24], turning back the shutter to its translucent state. The fall time is indicative of the change in the state from translucent to opaque. This is made possible by powering the shutter with sufficient voltage. The electrical torque causes the LC molecules to realign themselves parallel to the electric field. Thus, the rotation of the polarized light is blocked, causing the shutter to turn opaque.

The rectangular shutter has a rise and fall time of 8.7 ms and 3.5 ms respectively as shown in Figure 4.3. The rise and fall times for the circular shutter are 17.6 ms and 11 ms as shown in Figure 4.4. From Figure 4.5, we observe the rise and fall time of the video shutter to be 2.9 ms and 1.8 ms respectively. Table 4.1 summarizes the values of the three shutters under test.

The response time values are 6.1ms (rectangular), 14.3 ms (circular) and 2.4 ms (video) respectively. The reciprocal of the response times results in

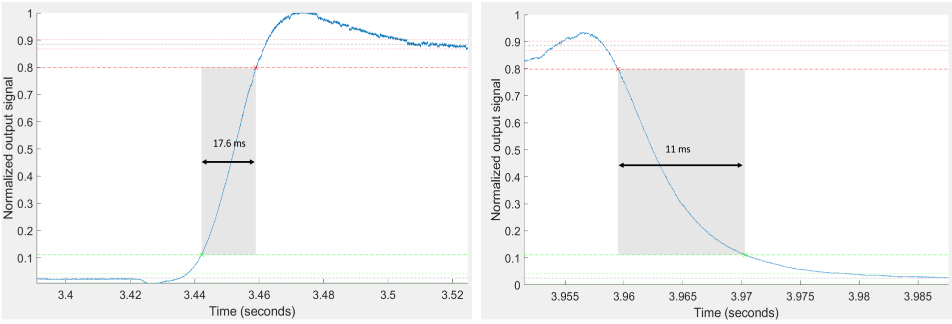

(a) Rise time

(b) Fall time

Figure 4.4: Rise and fall times of the circular shutter at 5V.

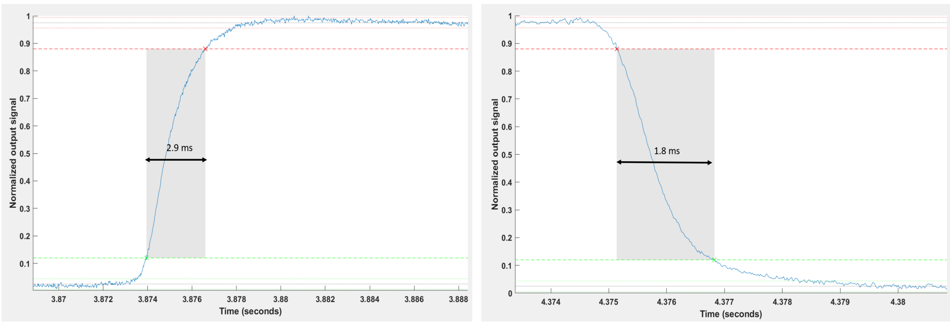

(a) Rise time

(b) Fall time

Figure 4.5: Rise and fall times of the video shutter at 5V.

Material	**Rise time (ms)**	**Fall time (ms)**	**Average response time (ms)**
Rectangular shutter	8.7	3.5	6.1
Circular shutter	17.6	11	14.3
Video shutter	2.9	1.8	2.4

Table 4.1: Response time measurements of the shutters driven at 5V.

the operating frequencies of 164 Hz, 70 Hz and 417 Hz respectively. These values represent the upper limit of the switching speed.

In each of the above cases, we observe that the fall time is shorter than the rise time; mainly because the fall time can be controlled by varying the supply voltage. The rise time is not electrically controlled and is influenced more by the material composition.

4.4 Effect of voltage on the response time

To understand the effect of the supply voltage on the response time especially the fall time, the experiment is repeated for varying voltages.

Driving the shutters at 3.3V

The microcontroller pin output voltage is 3.3V and is chosen as the supply voltage for measuring the response time of the three shutters. Table 4.2 gives an overview of the experiment.

Material	**Rise time (ms)**	**Fall time (ms)**	**Average response time (ms)**
Rectangular shutter	45	12.4	28.7
Circular shutter	13.7	35	24.4
Video shutter	3.3	4.8	4.1

Table 4.2: Response time measurements of the shutters driven at 3.3V.

The upper bound of the operating frequency (maximum data rate) for each of the shutters is computed as shown in Table 4.2. These values are 35 Hz, 41 Hz and 244 Hz for the rectangular, circular and video shutter respectively. The fall time is shorter than the rise time in case of the rectangular shutter, indicating that the shutter is switching close to its maximum opacity. However, this is not observed while driving the circular and video shutter at 3.3V. For the shutter to turn opaque, the voltage supplied should exceed V_{th} as discussed in 4.2. This is not the case with the circular shutter (V_{th} = 3.5V), resulting in it taking longer to turn opaque with the fall time being 2.5 times that of the rise time. The video shutter supply voltage does exceed its V_{th} of 2.3V, but is still not sufficient for reaching its maximum opacity as shown in Figure 4.2, with a fall time 1.45 times more than the rise time.

From Section 3.2, we know that the rise time of the shutter is dependent on the elastic torque to attain translucency. While switching at low voltages (particularly lower than V_{th}), we do not achieve white to black contrast as the maximum opacity is not reached. We can term this to be white to gray switching as the time taken to transition between these states is high due to voltage insufficiency. Thus, the response time is higher. However, from Figure 4.2, we can hypothesize that at higher voltages the switching will be be from white to black. This implies sufficient voltage to attain maximum opacity and in turn, reducing the response time of the shutter.

Driving at higher voltages

The response time of the LC shutter decreases with the supply voltage; thus enabling a higher contrast in the received signal. This hypothesis is based on the results of the previous experiments and are further validated by powering the shutters at voltage higher than 5V. The maximum voltage to drive a rectangular shutter is 5V, while the upper limit for the circular shutter is 15V and is undefined in case of the video shutter (the manufacturers recommendation is 10V+), making them suitable candidates for this experiment.

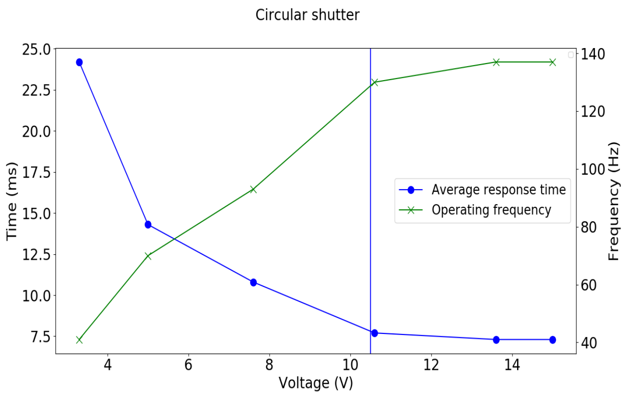

(a) Circular shutter

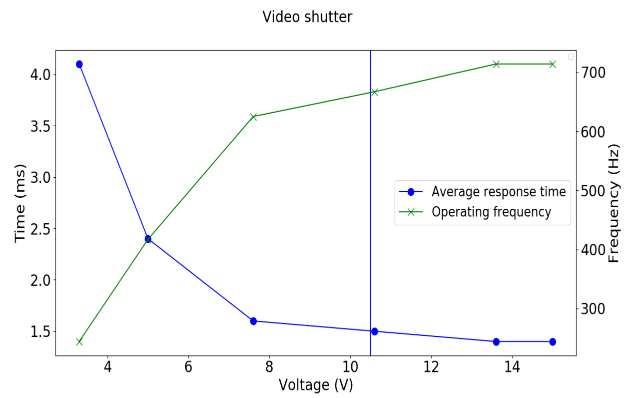

(b) Video shutter

Figure 4.6: Response time and the corresponding upper bound for the operating frequency.

Figure 4.6 shows two graphs, each representing the average response time and the corresponding upper bound of the operating frequency for voltages ranging from 3.3V to 15V respectively. The response time keeps decreasing till the voltage reaches V_{sat} after which, there is no further decrease in its value as shown by the vertical blue line in Figure 4.6. We also observe that the maximum operating frequency increases with voltage and is constant after V_{sat} as indicated by the vertical blue line.

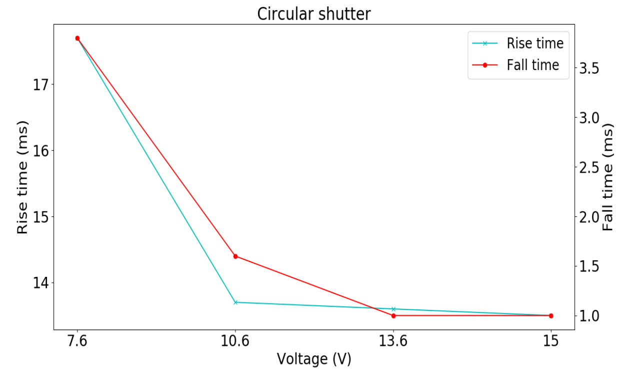

(a) Circular shutter

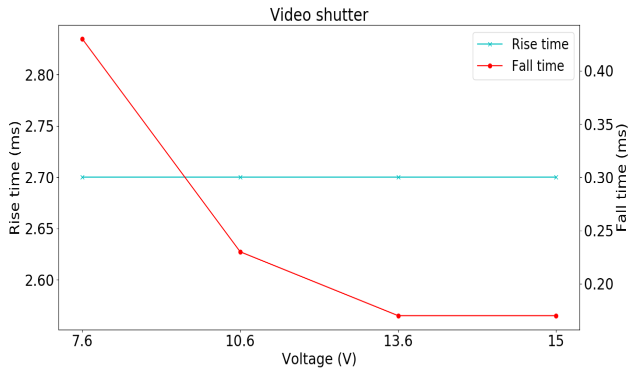

(b) Video shutter

Figure 4.7: Rise and fall times at varying voltages.

The fall time decreases with the voltage for both the shutters. However, the rise time decreases for the circular shutter and is a constant for the video shutter as shown in Figure 4.7. The dependency of the rise time on the material composition and the restoring (elastic) torque influences the observed trend, and hinders with further reduction in the response time. The response time can further be reduced by decreasing the cell gap i.e. the gap between the electrodes shown in Figure 3.2. The contact area between the LC and the substrate can be increased to reduce the rise time. This will enable faster relaxation while transitioning to the translucent state [11]. The material design changes suggested above can help to achieve lower response times, but is out of scope of this thesis.

From all the measurements, we observe that the rectangular shutter has a maximum calculated operating frequency of 164 Hz at 5V, higher than 137 Hz for the circular shutter at 15V. The response time measurement concludes that, out of the two shutters, the rectangular one is a better alternative as it has a high operating frequency at a low voltage. Overall, the operating frequency of the video shutter is 417 Hz at 5V which is twice in comparison to the other shutters. Also, the difference in the material design for each of the TN shutters is influential for the variation in the response time. Based on the above analysis, we can conclude that, the best material for the transmitter is the video shutter.

4.4.1 Verification of operating frequency

Section 4.4 provides the values of the maximum switching frequency computed with response time measurements for the three shutters under test. This requires experimental verification before establishing the permissible data rates for communication. The main objective in here is to validate these claims by amplitude measurements. The shutter is continuously toggled at varying frequencies for voltages in their respective operating ranges with a similar test setup. A Fast Fourier Transform (FFT) is performed on the received signal to observe the frequency components present in the received signal and verify if the dominant frequency is equal to the transmitted signal. After confirming the signal reception, the amplitude of the received signal is measured for the given transmission frequency.

The amplitudes are computed at varying voltages of each shutter, and then normalized with the corresponding maximum and minimum values from all the measurements. Figure 4.8 shows the heat maps representing the normalized amplitude variation in the received signal for varying frequency and voltages for the shutters under test. High amplitude signals are represented by shades of green, transitioning to lower amplitudes in shades of red. The upper frequency limit to the toggling is set by the maximum operating frequency measured at 5V for each shutter where, the amplitudes are indicative of the strength of the received signal. The rectangular shutter at 3.3V (5V) can switch up to 160 Hz, which is 4 times (equal) the computed frequency limit of 41 Hz (164 Hz). On the other hand, the circular shutter at 3.3V (5V) can switch up to 120 Hz, that is 3 times (1.7 times) its computed value in Section 4.3. The video shutter exhibits similar behavior by operating till 410 Hz, and is 1.68 times (1 time) higher than that calculated for 3.3V (5V). However, when the shutters switch very close to these frequency values, the signal amplitude is very low making decoding difficult. Thus, the maximum switching speeds are limited to values below this upper limit.

The heat map leads us to two main observations. The signal amplitude decreases with an increase in the frequency for a given voltage value as shown by the vertical transition from green to red in Figure 4.8. The amplitude values are indicative of the signal contrast observed for the given frequency

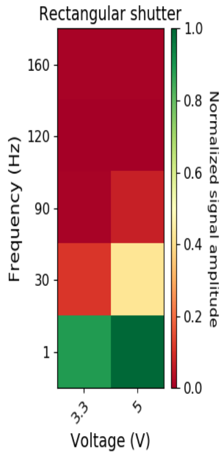

(a) Amplitude variation of rectangular shutter

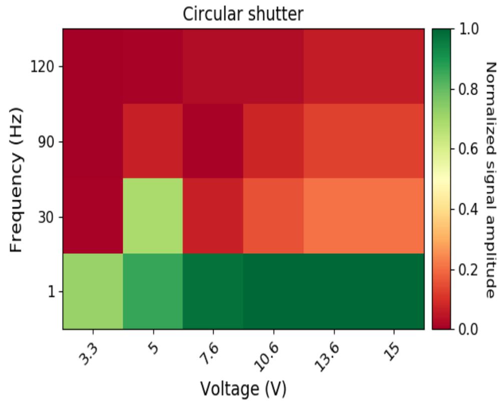

(b) Amplitude variation of circular shutter

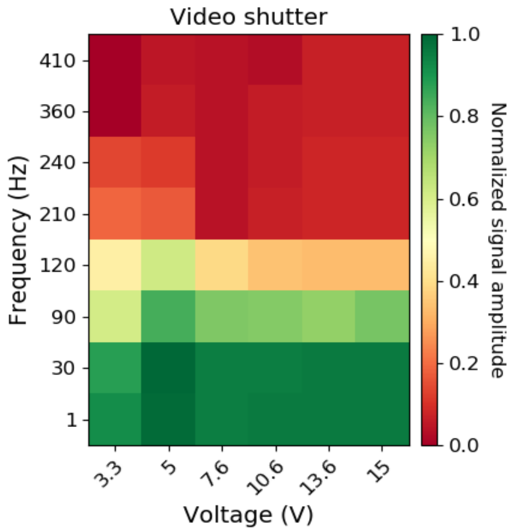

(c) Amplitude variation of video shutter

Figure 4.8: Signal amplitude for varying voltage and frequency values.

value. The decrease in the amplitude indicates that the transition is not from translucent to opaque, but is somewhere between the two. This can be referred to as light gray to dark gray transition. The LC molecules have insufficient time to attain complete relaxation (translucency) or total re-alignment parallel to the electric field (opaque). This is because, at high frequencies the LC shutter starts switching very close to its maximum permissible speeds causing the light gray to dark gray transitions.

The second main observation is that, the signal amplitude at a given frequency, for varying voltage values increases with an increase in the applied voltage. This can be seen by the horizontal color transition in the heat map. The higher voltages enable the LC molecules to attain maximum parallelism to the electric field, enabling improved opaqueness. However, at high frequencies this increase in the signal amplitude is not very distinct i.e., the signal contrast shows minimal improvement and the amplitude value is very low. This indicates that the LC molecules cannot be aligned any more parallel than it is for these frequency values; thus limiting the signal contrast. The amplitudes of the signals at higher voltages and frequencies are not significantly different to the corresponding low voltage case. This shows that, the shutters will have very low amplitudes at even higher frequencies, making it safe to limit it to the same maximum operating frequency value for all voltages.

The observations made based on the heat maps verify the claims made in Section 4.2 and 4.4 respectively. The heat map also shows that, the previously computed maximum frequency values at high voltages (5V+) for the circular and video shutters are not met. This is due to the signal amplitudes showing insufficient contrast at 120 Hz and 410 Hz respectively. Thus, from the experimental results, we can state that the maximum operating frequency for the rectangular, circular and video shutters are within 160 Hz, 120 Hz and 410 Hz respectively.

Chapter 5

Modulation and Coding

This chapter focuses on implementing a modulation scheme suitable for transmission using the LC shutter. The schemes deemed suitable for artificial light based communication are tested on these shutters. The responses are analyzed to test its feasibility on these materials. The main objective here is to select a modulation scheme that minimizes the flickering effect observed while transmitting light signals.

5.1 Data transmission

Chapter 4 analyzed the material for its maximum switching speed. The next step in the design process is to implement a modulation scheme suitable for data transmission using the LC shutter. Modulation is a process that causes a detectable change in the signal, enabling data transmission. The two major obstacles that occur in VLC with artificial lighting are flickering and dimming. Flickering is observed when the signal changes from one state to another i.e. when the light switches between on and off states, while dimming is implemented to improve energy efficiency. The major focus is to mitigate the flickering effects owing to its implications on human health. The IEEE 802.15.7 standard [19] describes the modulation schemes suitable for alleviating both these effects and are deemed to be suitable for LED lights (artificial light). LEDs, have low response times (high switching speeds) and can be toggled more efficiently with additional driver circuitry. In comparison, LC shutters are slower with high response times and different physical behavior; thus, exhibiting flickering. For proof of concept, the analysis in this chapter is only performed on the rectangular and the video shutter. The circular shutter has high response times, resulting in a maximum operating frequency of only 140 Hz at 15V, making it an unsuitable candidate.

Flickering can further be categorized into two types: inter-frame flicker and intra-frame flicker. A frame (here) refers to the transmission of a data

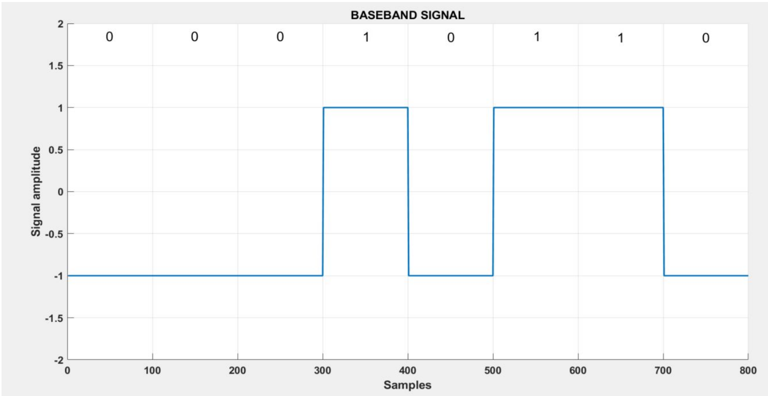

Figure 5.1: Baseband signal representation - OOK.

sequence. Intra-frame flicker is observed while transmitting a single data frame whereas, inter-frame flicker is spotted while transmitting two or more different frames. The primary objective here is to eliminate both types of flickering. To do so, we start with eliminating intra-frame flickering (hereon referred as flickering). This is analyzed by sending a pre-determined data payload of decimal 22, representing the ASCII synchronization character. It is transmitted in its 8 bit binary form of 00010110 and Figure 5.1 is a baseband representation of the same. This payload is chosen because it represents all four possible binary pairs: 00, 01, 10, and 11 respectively. The next sections focus on evaluating various modulation schemes and selecting the most suitable one for the LC shutter.

5.2 On-Off Keying (OOK)

OOK is a modulation method where the signal toggles between low and high states to represent binary zero and one respectively. It is a common and easy approach to modulation and is essentially transmitting the baseband signal. The transmitted signal should have equal number of ones and zeros to have a DC balance between them. The DC balance ensures consistent brightness of about 50% throughout the transmission. However, data streams can have unequal number of zeros and ones as shown in Figure 5.1, creating a DC offset. Thus, there is flickering due to uneven brightness during transmission. This can be tackled by transmitting at high frequencies. We know that, high frequency transmission is a limitation while using the LC shutter, making OOK an infeasible alternative to flicker free transmission.

5.2.1 OOK with Manchester coding

Flicker free transmission can be made possible when the DC offset is zero for data streams with unequal number of zeros and ones. Implementing Run Length Limited (RLL) coding schemes will solve this problem. RLL coding is implemented when there are bandwidth limitations (as in our case) and is useful when the number of consecutive zeros and ones in a sequence need to be controlled.

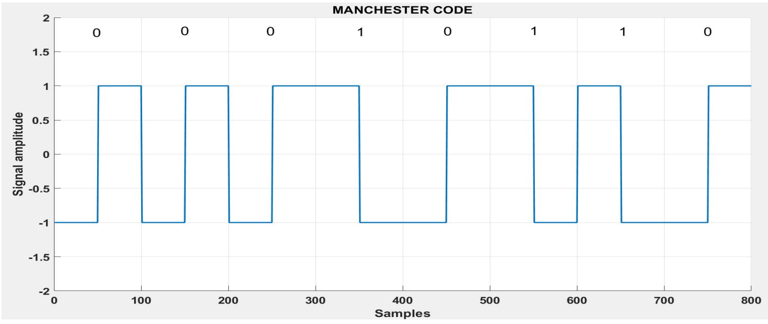

(a) Manchester code

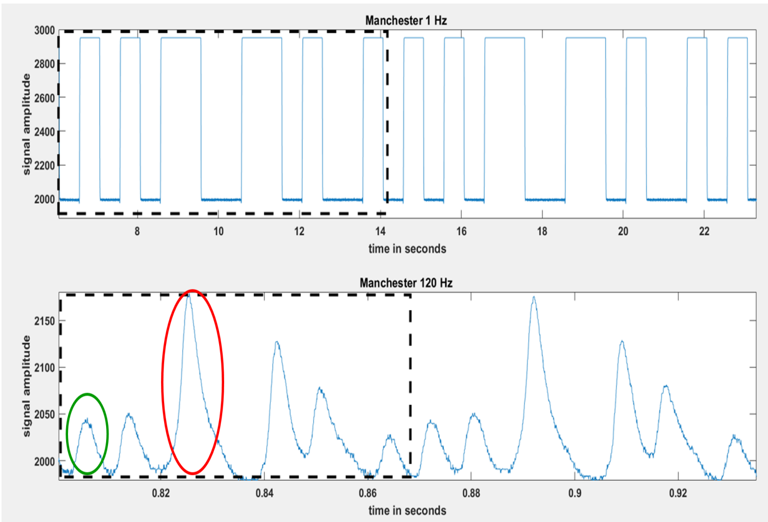

(b) Received signal at rectangular shutter

Figure 5.2: OOK with Manchester coding - Rectangular shutter.

OOK is implemented with Manchester coding, a form of RLL code. Here, each bit is comprised of two symbols: bit zero is sent as 01 and bit one is transmitted as 10 as shown in Figure 5.2(a). Transmitting bit zero as 10 and bit one as 01 represents inverted Manchester coding as shown in Figure 5.3(a). There are two types of transmissions sequences; one with a narrow pulse width (50% of bit duration) and the other with a wider pulse width (100% of bit duration) shown by the green and red circles in Figure 5.2(b). Here, the transmission comprises of only 1-2 consecutive symbols of the same type, limiting the pulse width. The data is detected by the mid bit transition as opposed to detecting at the start of each bit in case of OOK. This results in easier decoding of the signals in comparison to OOK as there are no long consecutive bit sequences.

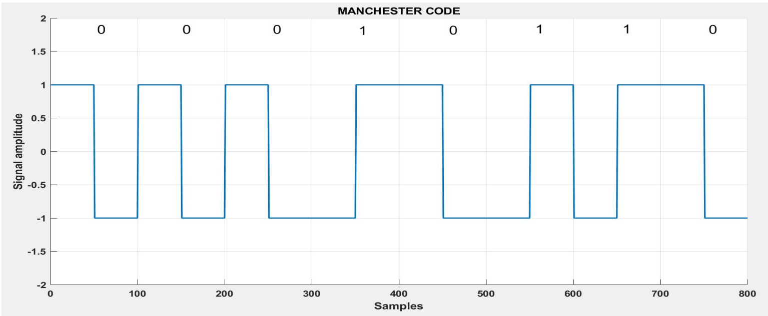

(a) Inverted Manchester code

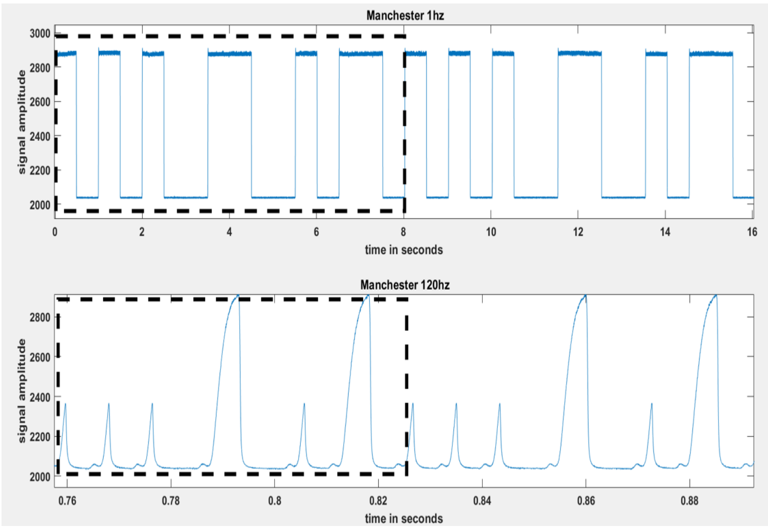

(b) Received signal at video shutter

Figure 5.3: OOK with Manchester coding - Video shutter.

The narrow pulses have lower amplitudes as opposed to the wide pulses at high frequencies as shown in Figure 5.2(b) and 5.3(b) respectively. The dotted black box represents a single transmission sequence at the given frequency. This amplitude levels are unequal for the transmission sequence, resulting in visible flickering at higher frequencies (120 Hz) as well. We observe that the width of the narrow signals are insufficient to achieve the same amplitude level due to the slow rise time of the shutters.

Along with the behavioral limitations, the Baud rate (number of symbol transitions) and data rate (bit rate- the speed of transmission) play an important role in determining the suitable modulation scheme. In this case, each bit has two symbols, resulting in a baud rate twice that of the data rate. The bandwidth is dependent on the baud rate. Thus, OOK with Manchester coding has a bandwidth twice of that seen in OOK. OOK with Manchester coding does not alleviate the effects of flickering and doubles the bandwidth requirement. Thus, it is an unsuitable data transmission scheme for the LC shutters. However, the variation of the amplitude based on the width is a cue to analyze this behavior of the shutter for flicker-free modulation.

5.2.2 OOK with Miller coding

The main drawback of Manchester coding was the unequal signal amplitudes which is reasoned to be because of narrow pulse widths. The amplitude inconsistencies are tackled by sending pulses wider than the ones sent in Manchester to have higher signal contrast and minimum amplitude variation. For the coding scheme, the symbol sequence for the current bit is determined based on the position of the previous bit. Bit 0 is coded as its previous symbol if the preceding bit is 1 and is inverted when preceded by bit 0. The first symbol of bit one is coded similar to the previous symbol, and the next symbol for the same is inverted as shown in Figure 5.4(a) and 5.4(b) respectively.

There are 2-4 consecutive symbols of the same type (zeros/ones) in this implementation. The number of consecutive symbols indicate the width of the signal. The idea here is to have pulse widths for a time period greater than or equal to the bit duration. The assumption based from the Manchester implementation is that, the pulse duration will be sufficient for the signal to reach its maximum amplitude and will not rise any further. Thus, the signals in Miller coding are expected to have a minimum amplitude difference and reduced flickering as shown in Figure 5.4(d). However, this is not observed for the rectangular shutter shown in Figure 5.4(c). We observe that, the amplitude difference for the pulse widths are still similar to that observed in Manchester, resulting in flickering and disproving the assumption. However, the bandwidth utilization is improved as the minimum symbol width is equal to the bit duration. Thus, bandwidth overuse is solved without any relief from flickering. Thus, we scan state that OOK with Miller coding is also an unsuitable alternative for modulating with LC shutters.

Alternative approach to alleviate flickering

The persistent flickering can be addressed by introducing some physical changes to the transmitter. The analyzer (output polarizer), enables the user to observe the changes in the transmission of light due to varying signal amplitudes as shown in Figure 3.2. The flickering effects can be minimized

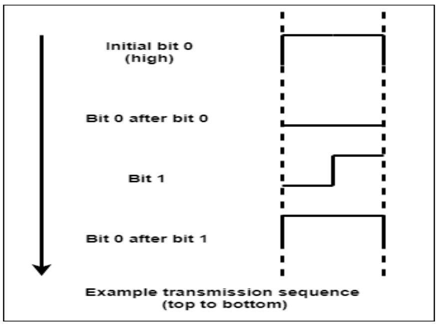

(a) Coding logic

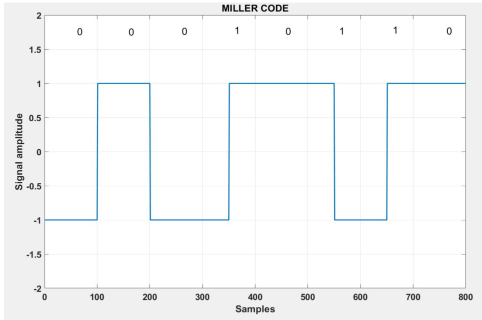

(b) Miller code

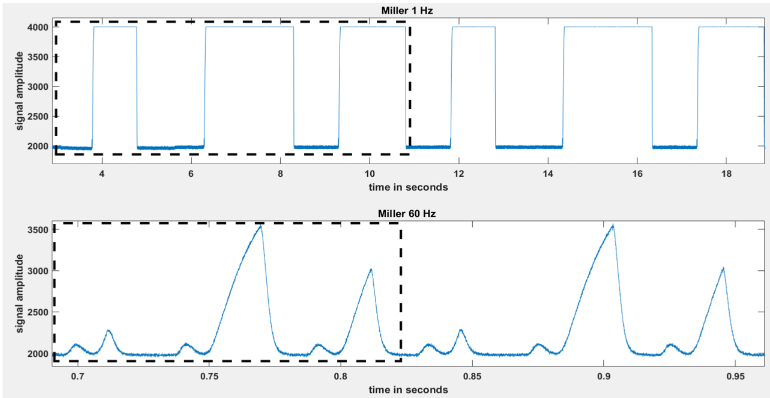

(c) Rectangular shutter

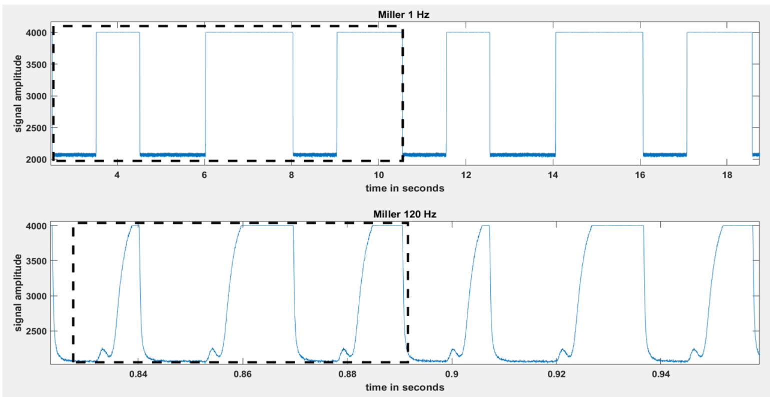

(d) Video shutter

Figure 5.4: OOK with Miller coding.

by removing the analyzer from the LC shutter and placing it at the receiver opening. Thus, the transmitter now comprises of a single polarizer and liquid crystal enclosed between two glass substrates. The received signal after this modification is shown in Figure 5.5(a). The amplitude inconsistencies are not visible to the naked eye; thus, flickering is reduced. However, at certain viewing angles, the flickering effect is minimally observed. Viewing angle is defined as the maximum angle for viewing a display without compromising on the visual performance as shown in Figure 5.5(b). This results in creating dependencies on the user orientation for observing flickering. This phenomenon can also be extended in case of OOK with Manchester coding. Repositioning the polarizer film minimizes observable flickering, but fails to completely eliminate it, and thus is a partially effective solution.

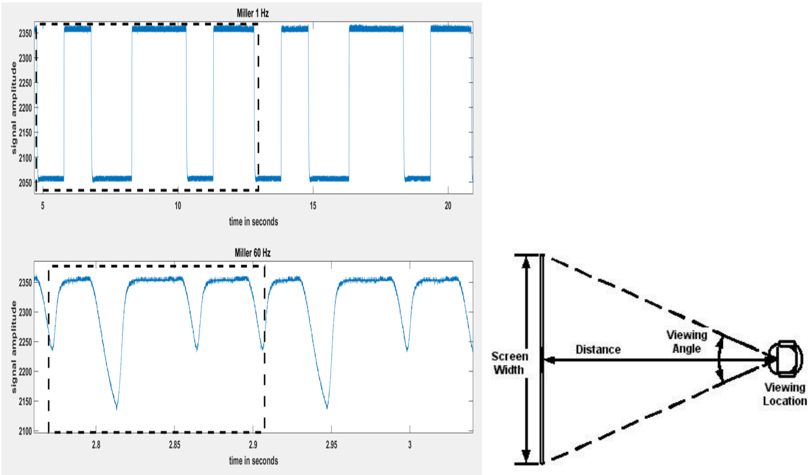

(a) Recieved signal (b) Viewing angle

Figure 5.5: OOK with Miller coding for rectangular shutter with the polarizer placed at the receiver.

Manchester and Miller coding have peaks of varying peak widths which result in varying amplitude levels resulting in flickering. The irregular peak widths are the cause of amplitude variation. This can be tackled by sending peaks of equal widths. Also, increasing the peak widths to allow more time to reach the maximum amplitude is not an effective alternative as seen in Miller coding. A better approach is to have more time between the peaks to enable consistency in the received signal amplitudes. The time duration (width) between the two peaks is varied as shown in Table 5.1. Here, T represents the bit duration, the columns represent the transition between the four possible bit combinations and the rows indicate the corresponding modulation scheme. Each column indicates the width between the two peaks for that particular transition. If the time duration is 0, as in case of Manchester and Miller coding, there is no interval between the peaks representing two separate bits. Thus, the high values of rise time makes it difficult to obtain clean transitions between the high and the low signals, resulting in varying amplitudes. The schemes with higher widths between their peaks are tested in the next sections of this chapter.

Modulation scheme	**0 –>1**	**0 –>0**	**1 –>0**	**1 –>1**
OOK + Manchester	0	0.5T	T	0.5T
OOK + Miller	1.5T/0	T	1.5T/0	0/T
OOK + Modified Miller	1.5T	0.75T	1.25T	0.75T
PWM (width 25% bit 0, width 30 % bit 1)	0.75T	0.75T	0.7T	0.7T
PPM (bit 0 - 0010, bit 1 - 1000)	0.25T	0.75T	1.25T	0.75T
PPM (bit 0 - 0010, bit 1 - 0100)	0.5T	0.75T	1.25T	0.75T

Table 5.1: Time duration between bit transitions for different modulation and coding schemes.

5.2.3 OOK with modified Miller coding

Modified Miller coding, a scheme used in NFC communication is implemented, where narrow peaks are transmitted to eliminate flickering due to amplitude variations. The received signal is low (opaque) for the entire bit duration when bit 0 is preceded by bit 1. It peaks for the first 25% of the bit duration when preceded by bit 0. Bit 1 transitions to a peak at 50% of the bit duration and lasts for 25% of the bit duration as shown in Figure 5.6.

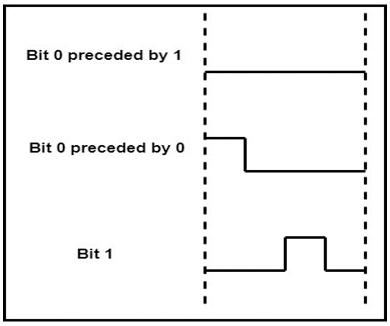

(a) Coding logic

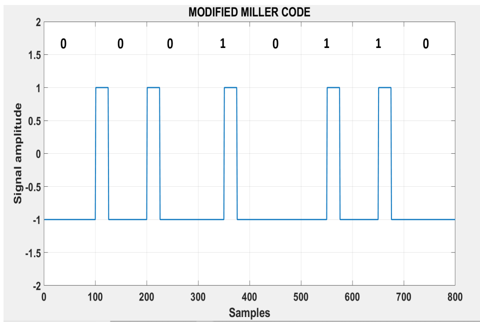

(b) Modified Miller code

Figure 5.6: Modified Miller coding for bit sequence 00010110.

The peak amplitudes are constant in this case due to the widths being equal. However, they are not equal with the number of bits transmitted as observed from the coding logic. As every bit is not coded with a peak, we do have a DC offset and minimal flickering is observed as compared to the previous schemes. This inequality is highly data dependent and can result in varying observations of flickering. In Miller decoding, the mid bit transition reveals if the bit is a one or a zero. However, in this case, a more complex logic is required for accurate decoding. This is because, a transition between the bit duration can either represent bit zero or bit one. Thus, the position

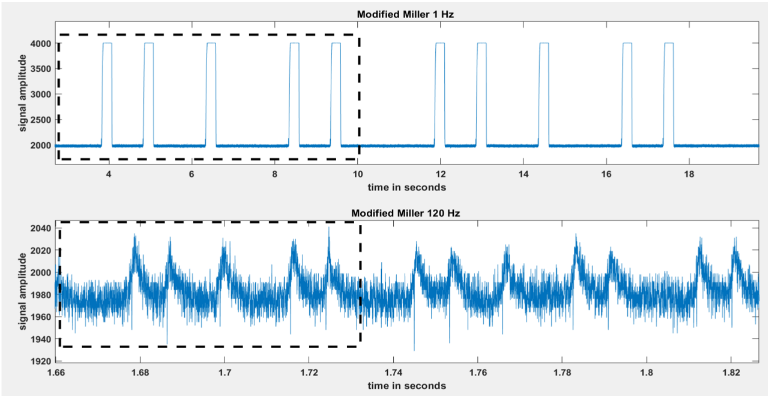

(a) Rectangular shutter

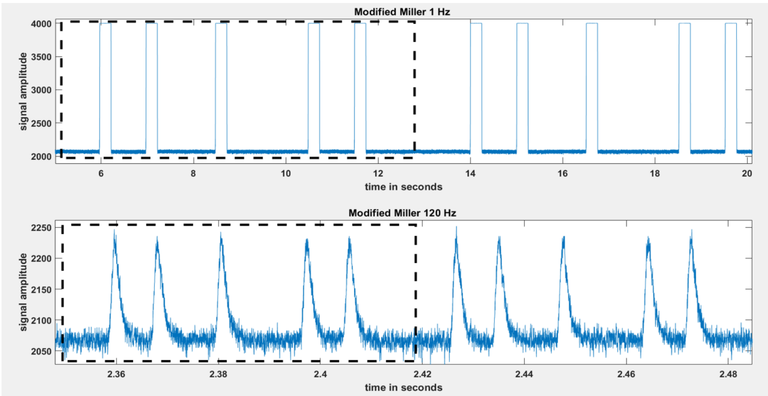

(b) Video shutter

Figure 5.7: OOK with modified Miller coding.

of the peak needs to be accurately mapped to decode the bit correctly. Thus, OOK with modified Miller coding minimizes the effects of flickering, and can be used more effectively by placing the polarizer at the receiver to further reduce the flickering effects.

5.3 Pulse Width modulation (PWM)

The difference between the number of peaks and the number of transmitted bits in modified Miller coding can be solved by implementing PWM. Pulse Width Modulation (PWM) is a method where the data is modulated with pulses of varying widths within the same pre-determined position for a given bit duration. The width of the pulses (duty cycle) determine the amplitude of the received signal. Based on previous implementations, we know that flickering is observed when pulses are wide and have uneven widths. If bit 0 has a duty cycle of D_0% and bit 1 has a duty cycle of D_1%, the transmission of a random bit sequence will cause a DC offset and cause flickering.

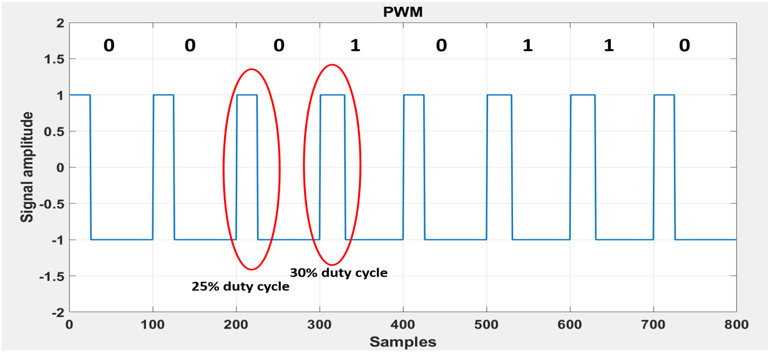

Figure 5.8: Pulse Width Modulation (PWM).

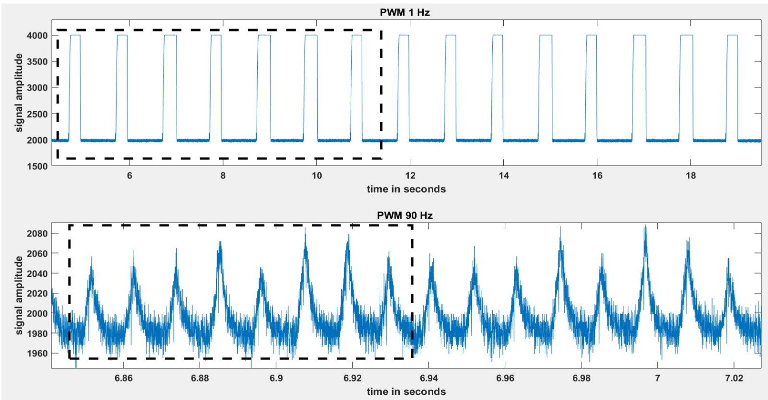

(a) Rectangular shutter

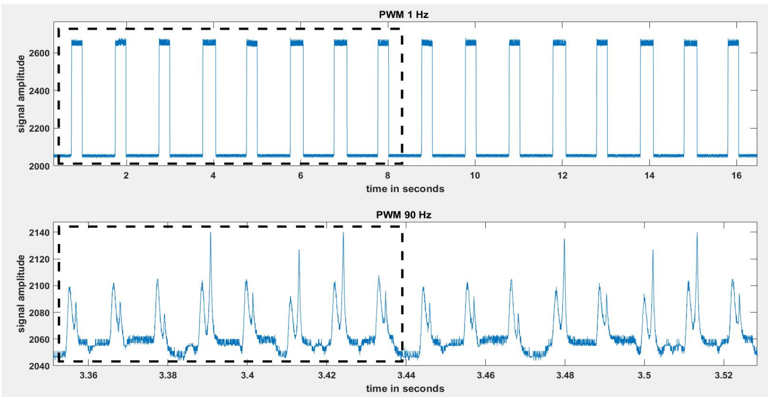

(b) Video shutter

Figure 5.9: PWM for 25% and 30% duty cycle for bit 0 and bit 1.

However, this can be minimized by reducing the difference between the

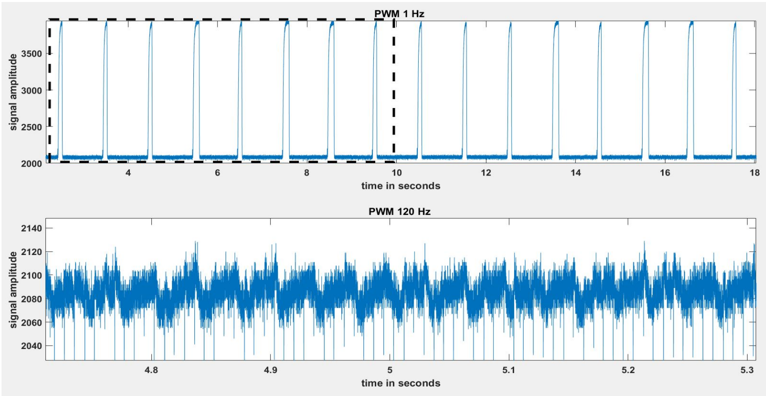

(a) Rectangular shutter

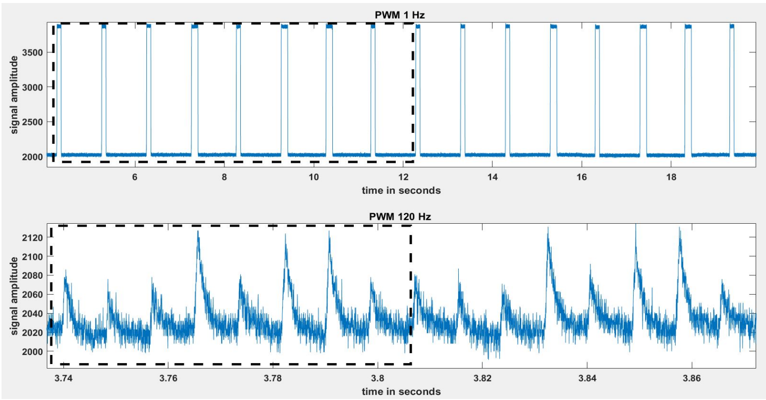

(b) Video shutter

Figure 5.10: PWM for 10% and 15% duty cycle for bit 0 and bit 1.

pulse widths to 5%. Also, having narrow pulse widths will give it more time for switching between the pulses as shown in Figure 5.9. Pulse widths of 25% and 30% duty cycle are heuristically chosen for transmission of bit 0 and 1 respectively as shown in Figure 5.8. We observe that, the amplitude variation is not very significant in case of both the shutters for this scheme, deeming it fit for modulating the LC shutter. However, the peaks have narrow widths, which indicates lesser time available for the shutters to switch to maximum transparency. Thus, The high rise time of the shutter results in the peaks having weak amplitudes and we observe noisy signals as seen for the rectangular shutter in Figure 5.9.

If the pulse widths are further reduced, the minimal amplitude difference observed previously can further be minimized. The duty cycle is further reduced to 10% and 15% for bit 0 and bit 1 respectively as shown in Figure 5.10. Flickering resurfaces as seen in case of the video shutter whereas, the rectangular shutter modulation results in very noisy signals. The pulse widths are very small for the shutter to peak within that time duration due to high response times, making it an unsuitable alternative. Switching at higher duty cycles will result in the same problem as observed in Manchester coding and will have insufficient time to transition between the two peaks. Since the duty cycle differences need to be small (5% in this case) to avoid flickering; it is difficult to have an error free decoding mechanism. Thus, PWM has reduced flickering at selective duty cycles, but is an unreliable modulation alternative for transmission using LC shutters.

5.4 Pulse Position Modulation (PPM)

PPM is a modulation scheme where the position of the peak is used to distinguish between the bits. Unlike PWM, the duty cycle in PPM is constant for a given bit duration. The DC offset is expected to be constant for a given transmission period; thus, enabling the shutter to transmit without any observable flicker. Here, bit 0 is modulated as a symbol sequence of 0010 and bit 1 as 1000 respectively. Figure 5.11 represents the expected signal reception and the widths between the peaks is as shown in Table 5.1.

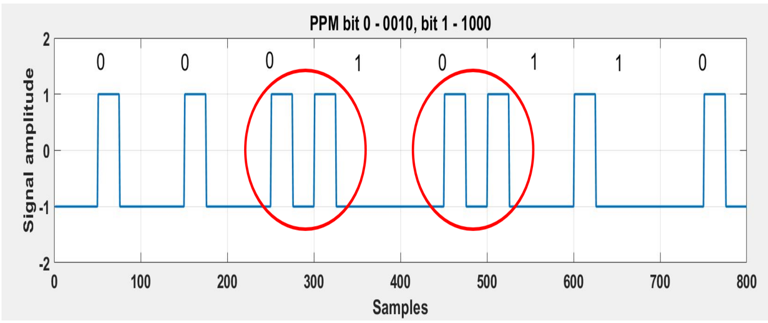

Figure 5.11: PPM type 1 - the minimum width between pulses is 25% of the bit period (shown by the red circle).

The 25% gap between the peaks of bit 0 followed by bit 1 is insufficient to attain the same signal amplitude for the peak. This results in minimal flickering at high frequencies as shown by the red circles in Figure 5.13. The width between the peaks is inadequate for the slow rise time of the shutters, as prominently seen in case of the rectangular shutter from Figure 5.13.

The width between the peaks can further be increased to tackle this issue. On modulation with a minimum peak gap of 50% of the bit duration i.e., bit 0 is sent as a symbol sequence of 0010 and bit 1 is sent as 0100 as shown in Figure 5.12. Here, we observe no flickering while transmission as shown in Figure 5.14. Thus, a minimum peak to peak gap of 50% is suitable to avoid significant amplitude variations.

PPM tackles the two major causes of flickering- the unequal pulse widths

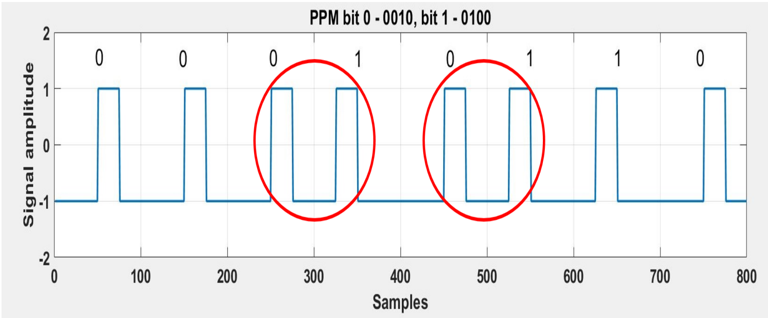

Figure 5.12: PPM type 2 - the minimum width between pulses is 50% of the bit period (shown by the red circle).

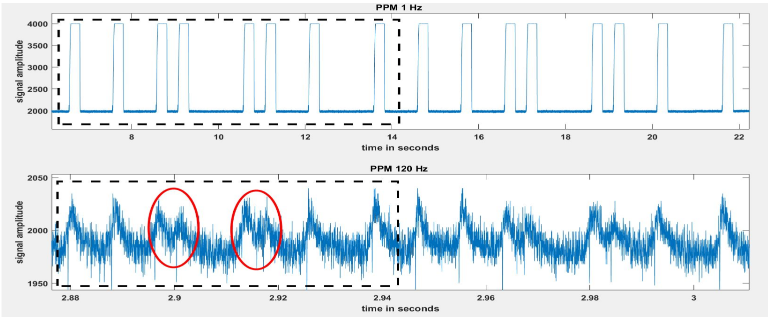

(a) Rectangular shutter

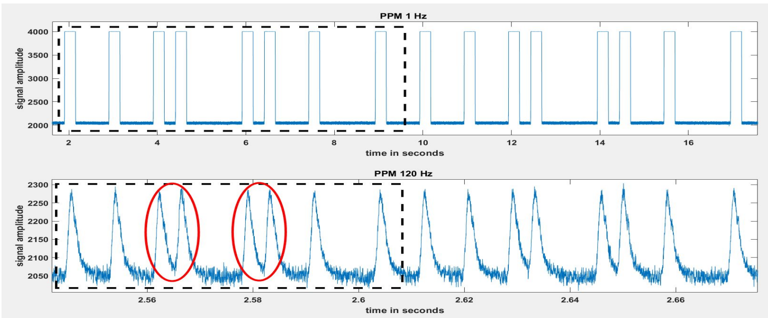

(b) Video shutter

Figure 5.13: PPM with minimum peak gap of 25% of the bit duration between two consecutive pulses.

leading to varying signal amplitudes, and the uneven number of peaks in a given bit sequence. Thus, PPM enables an intra-frame flicker free communication system without making any physical modifications to the LC shutter design. It is also expected to eliminate the overall effects of flickering (i.e. inter-frame flicker) and can be proved by conducting some visual experiments. An overview of each of the scheme under consideration is

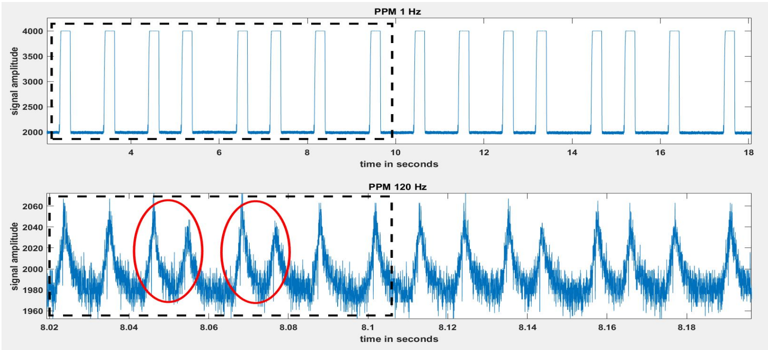

(a) Rectangular shutter

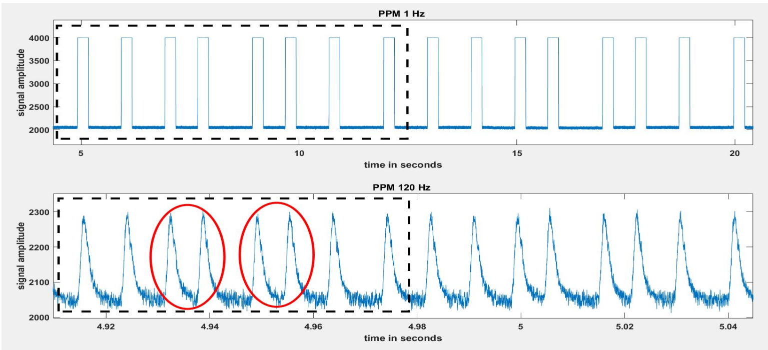

(b) Video shutter

Figure 5.14: PPM with minimum peak gap of 50% of the bit duration between two consecutive pulses.

shown in Figure 5.15. PPM is suitable for shutters with low or high rise times and thus, is a good modulation choice while communicating with an LC shutter.

Visual evaluation

The evaluation for choosing a flicker free modulation scheme was performed based on observing the received signals for their amplitude values. This analysis resulted in choosing PPM as the best alternative for modulating the LC shutter. However, the essence of the thesis being sunlight based communication, the reduced flickering observed by implementing PPM is further verified by testing it in sunlight. A visual evaluation experiment is conducted on 10 candidates, where the rectangular and video shutters transmit data at varying frequencies. Unlike the previous test cases, a random data stream is transmitted to observe the overall effects of flickering on the human eye. The candidates rate the visual disturbance for each of the test cases that vary in their operating frequencies. The experiment was

Modulation/ coding scheme	Number of symbols per bit	Bandwidth	Flickering	Reason for flicker/ no flicker
OOK	1	Equal to baseband frequency	Very high	Average DC component not zero
OOK + Manchester	2	2 X baseband frequency	High	Varying signal amplitudes due to 1-2 consecutive similar symbols
OOK + Miller	2	Equal to baseband frequency	Reduced flicker after 90 Hz	Varying signal amplitudes due to 2 -4 consecutive similar symbols
OOK + Modified Miller	4	4 X baseband frequency	Reduced flicker after 30 Hz	Unequal number of peaks for the transmitted bit sequence
PWM	2	Depends on the pulse width	Reduced flickering after 30 Hz but persistent when the duty cycle is increased	The difference between the pulse widths has to be minimum to avoid varying signal peaks
PPM	**4**	**4 X baseband frequency**	**Reduced flickering after 30 Hz**	**Equal number of peaks with same amplitudes**

Figure 5.15: Comparison between the LC shutter modulation schemes.

performed on a overcast day with the light intensity ranging from 180 lux to 20,000 lux due to the movement of clouds in that period. Figure 5.16 and 5.17 shows the percentage of people rating the flickering based on the predefined test scale for the rectangular and video shutter respectively.

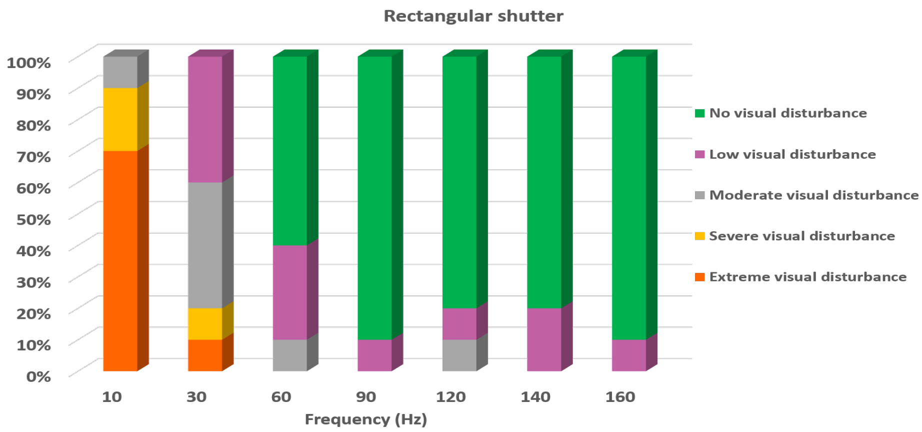

Figure 5.16: Visual evaluation results- Rectangular shutter.

In both cases, 60-70% of the candidates observed extreme visual disturbance while transmitting at 10 Hz. As the frequencies increased to 120Hz, 70-80% of the candidates observed no visual disturbance in both shutters. Along with individual perception, the lighting conditions highly influence the observation of flickering. The varying light intensities in some cases resulted in the 20-30% candidates observing low to moderate flickering. This can be compared to having a candle lit in a dark room. The flickering of the

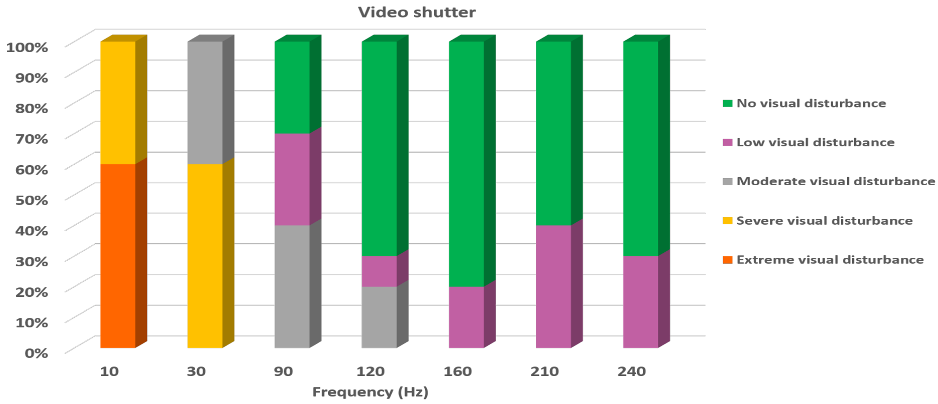

Figure 5.17: Visual evaluation results- Video shutter.

flame at a low frequency and is visually disturbing when viewed for long durations as opposed to candles lit in a room with sufficient natural/artificial light. The visual perception of every candidate is unique and influences their observations along with the lighting conditions. This can be extended to the case of the maximum computed frequencies of 160 Hz and 240 Hz for the rectangular and video shutter respectively, where 70-90% of the candidates observe no flickering.

Since the data transmission was a random bit stream, the results explain the observation of both inter and intra frame flickering. The visual evaluation experiment shows that the overall effects of flickering are minimized by PPM at frequencies greater than 120 Hz for both the shutters. The experimental and visual evaluation leads us to the conclusion that, PPM is a good modulation approach for sending data using LC shutters with low response times.

Chapter 6

System evaluation

This chapter focuses on understanding the influence of the LC shutter on the system parameters. Section 6.1 discusses the demodulation algorithm implemented for the captured light signals from the LC shutter. The data rate, communication range and other performance parameters are measured in Section 6.2.

6.1 Demodulation algorithm for PPM

From Chapter 5, we concluded that PPM is a suitable modulation scheme for LC shutters. The next step is to verify if the data can be transmitted till the maximum operating frequency computed in Chapter 4. This is performed by decoding the captured signals at the receiver to check if the data sequence is received correctly.

The LC shutter, when modulated using PPM, does not produce perfect square pulses [18]. Thus, a custom decoding scheme is designed based on the observed received signal. The demodulation is done offline after capturing the received signal and the system parameters are measured. The transmitted data stream is captured by the receiver with a sampling frequency of 50 kHz for a duration of 24 seconds. Figure 6.2 shows the algorithm used for decoding the signals. Since the transmission frequency is known beforehand, FIR filtering is performed on the downsampled received signal. This is done to eliminate high frequency noise components from the signal.

The next step is to set a threshold which will determine if there is a peak or not. The threshold is measured based on the amplitude of the received signal. To do so, the histogram of the amplitude values are plotted. The difference between the maximum and minimum value indicates the amplitude of the signal. The threshold is then set to 50% of the signal amplitude and the time duration of of the signals are measured. This value is chosen based on the visual observation of the signal and varies for different frequencies. For each sample, the signal amplitude compared to the threshold. The signal is classified as a peak (no peak) if it does (does not) cross the threshold value and the corresponding time duration is measured. For every bit, there is a peak present at different positions; 0010 for bit 0 and 0100 or bit 1 respectively. The ratio of the time duration between the peaks to that of the peak duration gives the number of zeros between the peaks as shown in Figure 6.1. Thus, the time duration of the signal between the peaks helps determine if the received data represents bit 0 or bit 1 respectively. A matrix indicating these ratios is created for the entire signal duration.

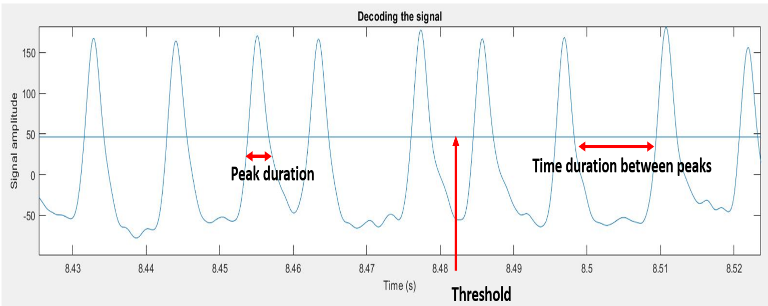

Figure 6.1: Signal measurements for decoding.

For the measurements in this section, the ASCII synchronization character (decimal number 22) is sent as a sequence of 8 bits- 00010110. It is common practice to send a bit stream prior to data transmission to establish communication between the transmitter and the receiver. For evaluation purposes, a continuous stream of the synchronization bit is sent by the transmitter. A sequence of 8 bits is represented by a set of 16 time duration values. Thus, a moving window of size 16 is used to decode the received data sequence. Since we have a continuous transmission of the same 8 bits, we can match the ratios computed signal duration to the expected signal duration and determine if the reception is accurate. The number of transmitted bits and received bits are computed and are used to calculate the BER.

6.2 Performance measurements

The system parameters and their influence are discussed in this section.

6.2.1 Bit Error Ratio (BER)

The Bit Error Ratio is defined as the ratio of the number of erroneous bits observed to that of the total bits transmitted as shown by Equation 6.1. The BER indicates the accuracy of data reception for a given modulation frequency. It used as a measurement index to detect the maximum modulating frequency and verify it with the theoretical measurements from Chapter 4.

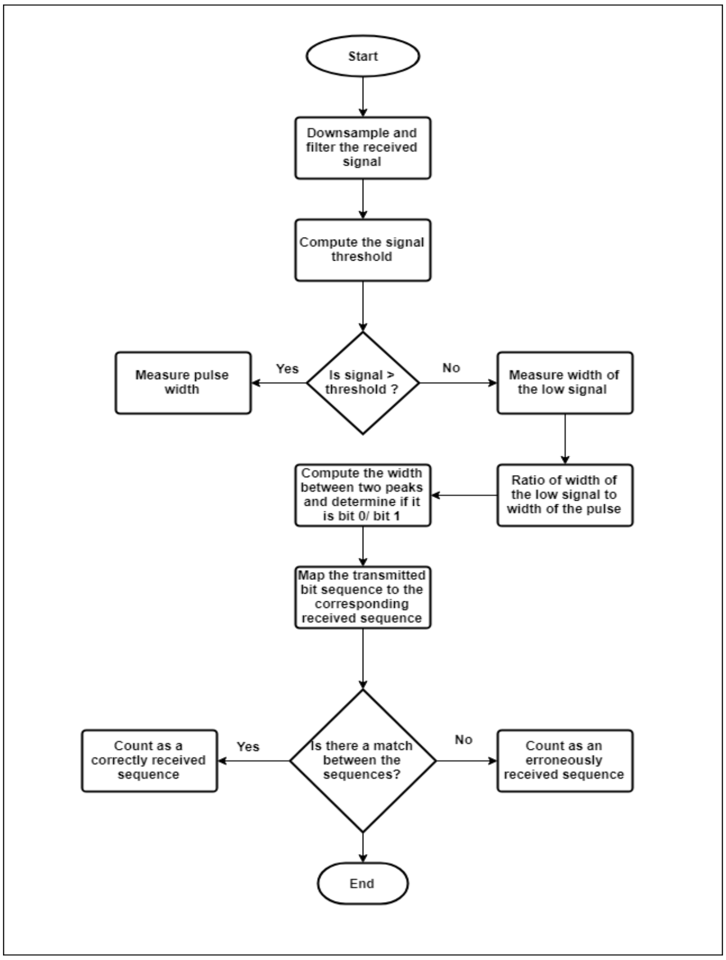

Figure 6.2: Flowchart representing the approach to demodulate the PPM received signals from the LC shutters.

$$BER = \frac{Number\ of\ bits\ in\ error}{Total\ number\ of\ transmitted\ bits} \tag{6.1}$$

The experimental setup is the same as the previous chapters. Here, a packet represents the ASCII synchronization character 22 and has a size of 8 bits. The packets are transmitted for a duration of 24 seconds. The number of packets varies based on the modulation frequency. The rectangular and video shutter are driven at 5V and 10.6V to obtain maximum contrast between the signals as shown in Chapter 4. The computed BER for the decoded data is shown in Figure 6.3.

The BER is 0 till 120 Hz and 160 Hz for the rectangular and the video shutter respectively. The BER shoots up to 55% and higher after 140 Hz (290 Hz) for the rectangular (video) shutter. Thus, the maximum switching

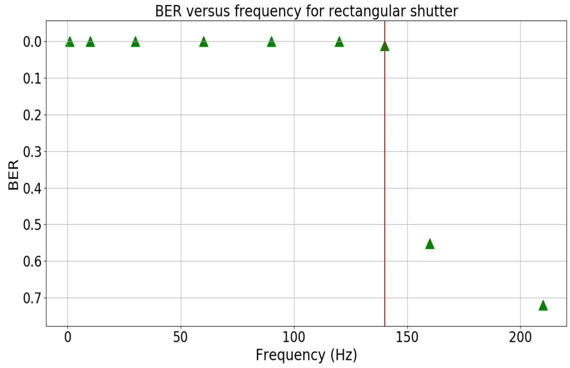

(a) Rectangular shutter - Theoretical maximum of 160 Hz.

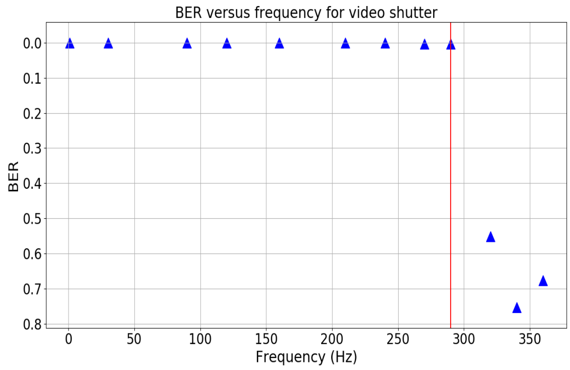

(b) Video shutter - Theoretical maximum of 660 Hz.

Figure 6.3: BER for varying frequency values.

frequency of the shutters are limited to these values as shown by vertical red lines in Figure 6.3. The BER is indicative of the decoding errors occurring in the received data stream. It is dependent on the operating frequency, lighting conditions, noise and the distance from the receiver. The minimal errors observed here can be solved by implementing suitable error detecting and error correcting codes.

The response time based computation for these shutters in Chapter 4 resulted in the maximum frequency for the rectangular (5V) and video (10.6V) shutters ranging at 160 Hz and 660 Hz respectively. While the rectangular shutter more or less meets this criteria, the video shutter switches at about half of this computed frequency. The objective here is to reduce the effects of flickering, which is satisfied by both shutters at 120 Hz and higher as shown in Figure 5.16 and 5.17 respectively. Thus, it can be concluded that that maximum data rate for the rectangular and video shutter are 140 bps and 290 bps respectively.

6.2.2 Orientation angle

There is a direct Line Of Sight (LOS) between the transmitter and the receiver while communicating with VLC. The transmitter and receiver are placed on a surface which is the XY plane. The transmitter is rotated on this plane at different angles as shown in Figure 6.4. The change in the angle of the transmitter will result in the variations in the received signal. For better visualization of this concept, the orientation angle is varied for the shutters at a modulating frequency of 30 Hz, and the BER is calculated.

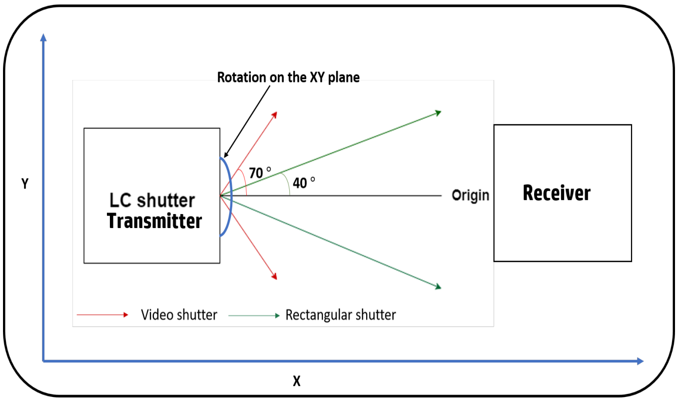

Figure 6.4: Orientation angle of the LC shutter with respect to the receiver.

Figure 6.4 shows the maximum orientation angle of the LC shutters for which data reception is not erroneous for the observed test case. The signal from the rectangular shutter is captured correctly till 40° at either side from the point of origin. When the angle is increased any further, the receiver is saturated by the incoming light (in this case, the DC light source) and the signal is not captured. This can be eliminated by controlling the light intensity entering the shutter either by using a polarizer to reduce the light intensity or by decreasing the size of the receiver opening. In case of the video shutter, this angle is measured to be about 70° from the point of origin. Figure 6.5 shows the received signals of both the shutters for varying angles. The BER for both the shutters is 0 at these angles, indicating the successful reception of data. The maximum orientation angle will vary with an increase in the modulating frequency. The maximum data rate will vary for different angles and need to be analyzed for higher frequencies.

6.2.3 Communication range

The communication range is indicative of the maximum distance up to which signals can be accurately detected at the receiver. The maximum detection area within the FoV of the receiver is calculated in [6] to get an estimate

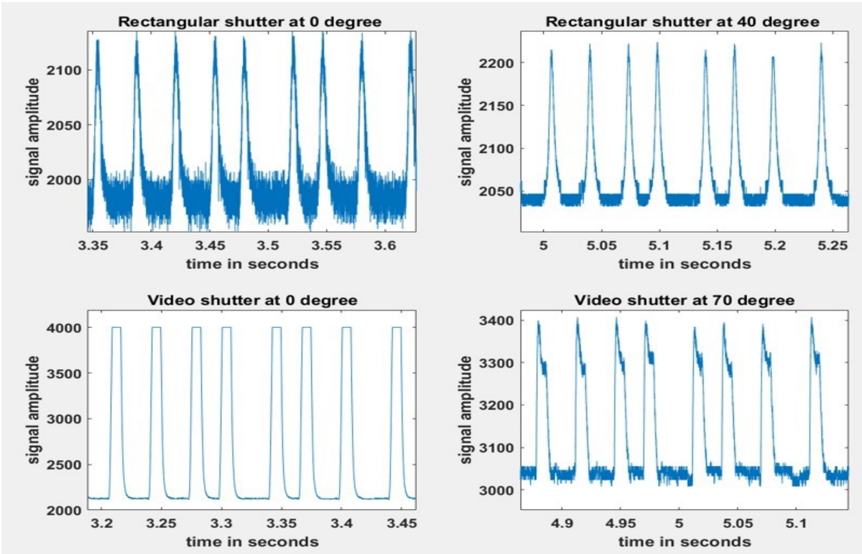

Figure 6.5: Received PPM signal for varying orientation angles of shutters.

of the barcode stripe width. This approach can be extended to measure the maximum communication distance of the LC shutter where the FoV of the receiver is entirely covered by the shutter. Here, the size of the shutter is known and the formula for the distance calculation is derived as shown in Equation 6.2. The size of the phototransistor and that of the shutter is represented by s_{pd} (1 mm) and A respectively. The size of the opening is represented by s_g (10 mm). The distance between the opening and the phototransistor is given by d_{pg} (54 mm) and that between the material and the opening is given by d_{mg} as shown in Figure 6.6.

$$d_{mg} = \frac{(A - s_g) \times d_{pg}}{(s_{pd} + s_g)} \tag{6.2}$$

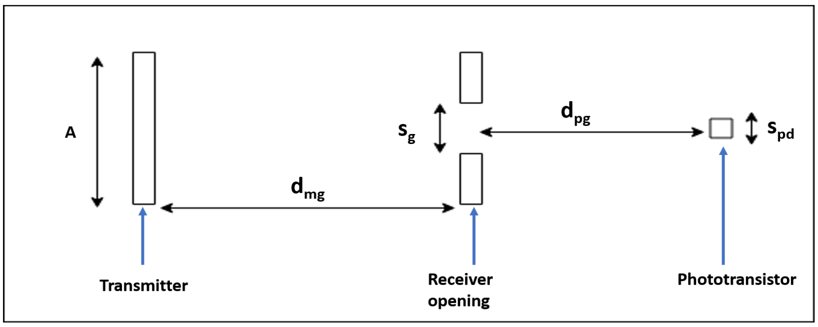

Figure 6.6: Parameters used for theoretical range calculation.

The geometrically computed distances for each of the three materials is shown in Table 6.1. This distance indicates that the entire FoV of the phototransistor is covered by the LC shutter. When the distance crosses this value, the signals captured will be noisy to to interference by unmodulated sunlight, making detection difficult. This interfering light is considered as a DC offset and can be removed electronically.

Material name	**size A (in mm)**	**distance d_{mg} (in cm)**
Rectangular shutter	38 mm	14
Circular shutter	110 mm	49
Video shutter	34 mm	12

Table 6.1: Geometrical calculation of communication range with s_g=10mm.

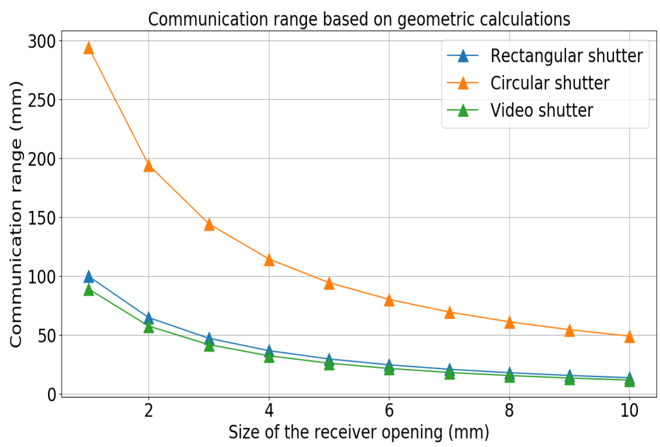

Figure 6.7: Computed value of communication range based on size of receiver opening.

The larger the size of the material (A), higher is the communication range as observed from Table 6.1. The communication range increases with a decrease in the size of the receiver opening s_g as shown in Figure 6.7. The decrease in the size of the opening indicates that less light would be captured and will result in noisy signals at higher frequencies. Thus, there is a trade-off between the communication range and the data rate.

The communication range is computed at 120 Hz for the rectangular and video shutters respectively. This value is chosen as it is the minimum operating frequency for flicker free transmission as shown in Section 5.4 . The size of the receiver opening is 10 mm. The distance between the transmitter and receiver is varied and the BER is computed. For the rectangular shutter, the data is received correctly till a distance of 45 cm after which, the received signal deteriorates and the detection becomes difficult. In case of the video shutter, this value is 105 cm at 120 Hz as shown in Figure 6.8.

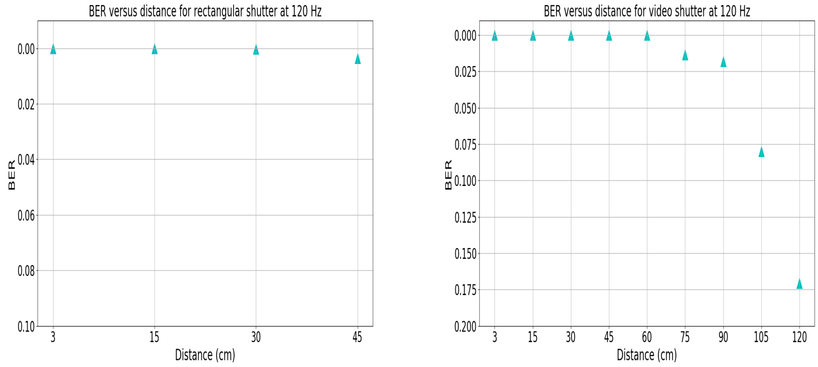

(a) Rectangular shutter at 120 Hz (b) Video shutter

Figure 6.8: Distance v/s BER at 120 Hz.

The communication distances are bound to decrease at higher frequencies and is about 45 cm for the video shutter at 240 Hz. Thus, for a minimum flicker free transmission frequency of 120 Hz, the maximum communication ranges are 45 cm (rectangular) and 105 cm (video) respectively. The range can be improved by reducing the size of the receiver opening and adding a lens at this opening to concentrate more light on the phototransistor. The communication range is very low with the small sized shutter as compared to BLE (Bluetooth Low Energy), which has a LOS range of 50 m.

6.2.4 Power consumption

Power consumption is another key parameter that needs to be measured while using an LC shutter as the transmitter. The current consumption of the shutter is dependent on the supply voltage, operating frequency and the surface area. The influence of each of the above on the current consumption is shown in Figure 6.9.

The graph represents the current consumption of the rectangular and video shutter at their best operating voltage. The vertical green line indicates the current consumption of the shutters at the minimum flicker-free modulating frequency of 120 Hz. The values of current drawn by the shutters are 68x10^{-3} mA (rectangular) and 59x10^{-3} mA (video) respectively. We observe that, the current drawn increases with an increase in the frequency but is less than 1 mA for the maximum computed data rates in Section 6.2.1, making it a competitive technology for energy efficient communication. It is observed that, the current drawn increases with an increase in the area as shown in Figure 6.9. The current is also dependent on the supply voltage as shown in Figure 6.10. Thus, an increase in the voltage value results in a higher current consumption.

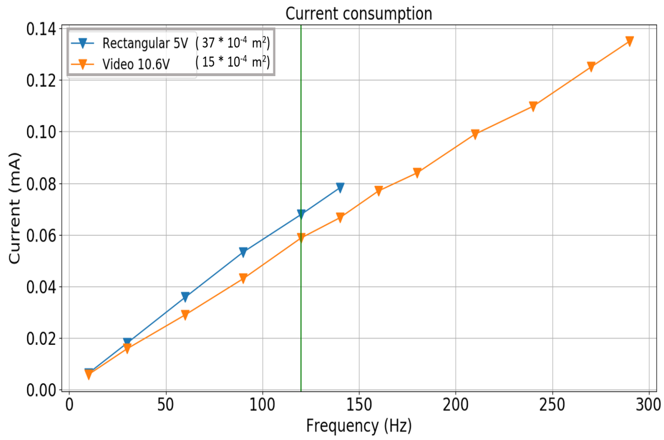

Figure 6.9: Relation between the frequency and current consumption for the shutters.

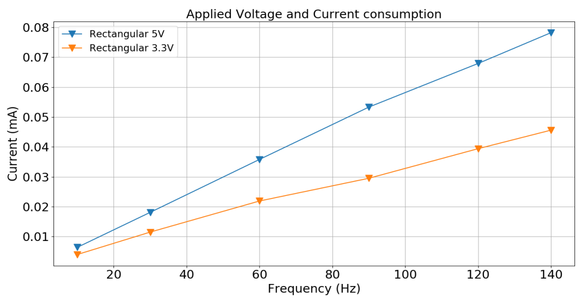

Figure 6.10: Relation between current consumption and supply voltage-Rectangular shutter.

The surge in the current caused by high drive voltages and high frequencies influence the power consumption of the transmitter. The power consumed per unit area for each of the shutters is as shown in Figure 6.11. At 120 Hz, the power consumption of the rectangular shutter is 46 mW/m^2 and 213 mW/m^2 for the video shutter respectively and is highlighted by the vertical blue line. The power consumption is lower than 500 mW/m^2 for the shutters at their maximum operating frequencies. The power consumption by the a shutter of 2 m^2 at 120 Hz is 43 mW/m^2 for the rectangular and 78 mW/m^2 for the video shutter respectively. A shutter of this size can communicate up to distances of 10 m as calculated from Equation 6.1. Thus, we observe that it is possible to transmit at long distances with low power consumption. On other hand,the BLE (Bluetooth Low Energy), when powered at 3.3V has a power consumption of about 84 mW when it is purely in the data transmission phase [22]. On comparing with this technology, the power consumption

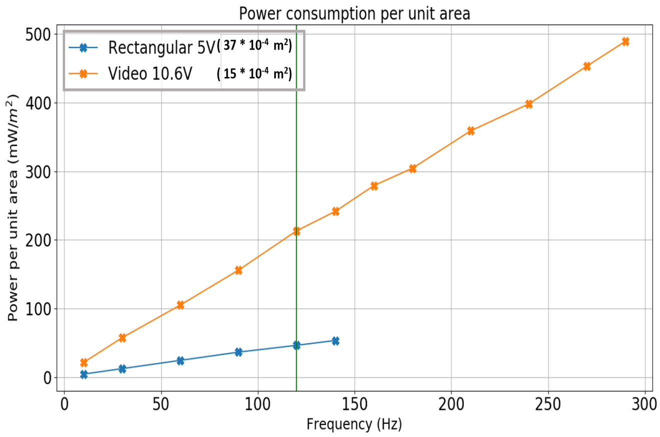

Figure 6.11: Power consumption per unit area.

of the small sized shutters at 120 Hz are 0.170 mW (rectangular) and 0.311 mW (video) respectively. The receiver power consumption is 6 mW. Thus, we have a trade off between power consumption and data rate when we compare to BLE. Table 6.2 summarizes the transmission parameters for the LC shutters. Table 6.3 gives an overview of the BLE performance parameters. From all the parameters, the power consumption of the LC shutter is comparable to BLE. Thus, the passive communication system has scope to function as a communication platform in parallel to the existing low power technologies.

Shutter type	**Maximum data rate (bps) at 30 cm**	**Communication range (m) at 120 Hz**	**Power (mW) at 120 Hz**
Rectangular	140	0.45	0.170
Video	290	1.05	0.311

Table 6.2: Summary of the LC shutter performance parameters.

Data Rate	**Communication range**	**Power**
1 Mbps	50m for LOS	84 mW

Table 6.3: BLE performance parameters [22].

6.3 Transmission in sunlight

The thesis aims to set up a communication system using sunlight. The efficiency of the LC shutter to work as a transmitter was tested in a controlled environment to benchmark these parameters.

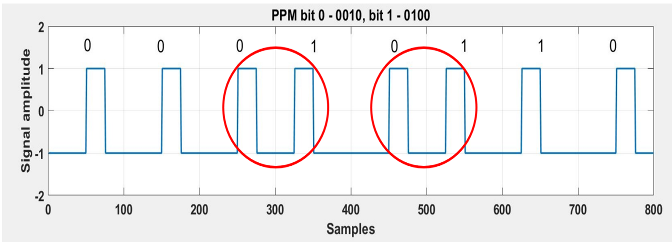

Figure 6.12: PPM for ASCII synchronization character 22.

To test the working of the transmitter in sunlight, PPM is implemented (Figure 6.12) and the ASCII synchronization character 22 is transmitted at a distance of 20 cm. The setup is near a window with direct sunlight and the measured light intensity during the course of the experiment is between 3200 lux 25,000 lux. To understand the working of the setup in sunlight, it is tested at the minimum flicker-free frequency of 120 Hz. Figure 6.13 shows the graph of the received signal for both shutters and the corresponding power spectral density.

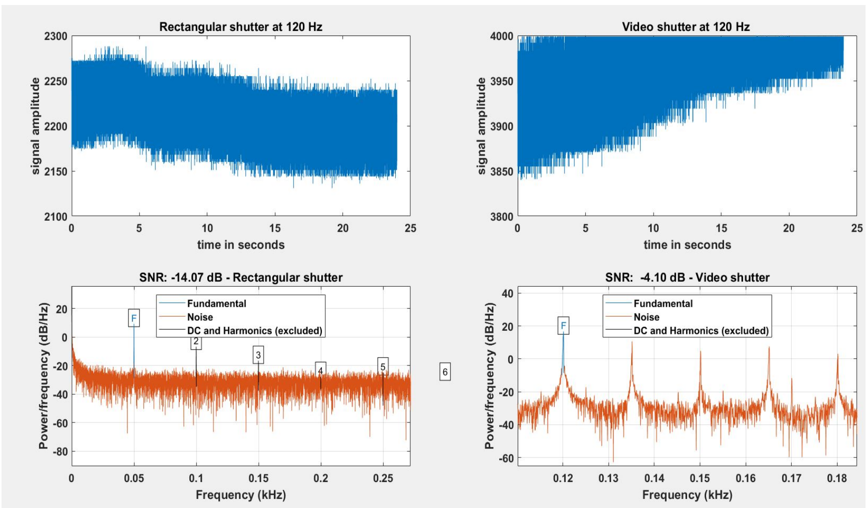

Figure 6.13: Received signal and power spectral density of the shutters.

There is a DC offset caused by unmodulated sunlight resulting in a trend in the signal amplitude levels. Secondly, there is no peak peak at 120 Hz, clarifying that the signal has not been received correctly due to interference from the surroundings. In addition, we know from Section 6.2.3 that, the rectangular (video) shutter will have interference from unmodulated sunlight when the distances are greater than 14 cm (12cm). Thus, the external environment influences the received signal in comparison to the signal received in the dark room as shown in Figures 6.14 and 6.15. The dotted box indicates a single transmission sequence (packet).

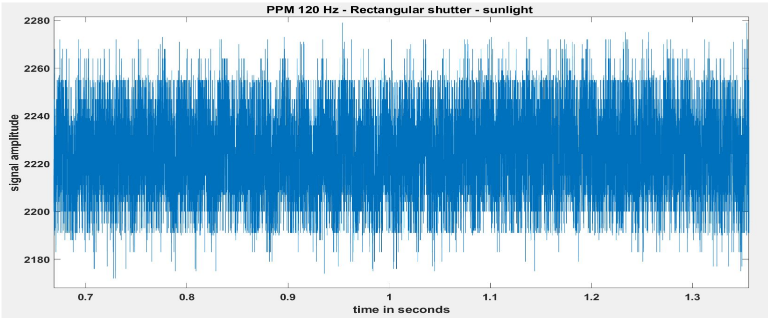

(a) Rectangular shutter - sunlight - not received

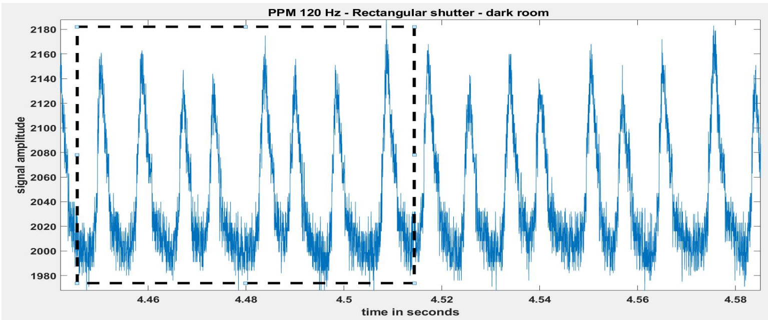

(b) Rectangular shutter - in dark room

Figure 6.14: PPM signal transmission at 120 Hz in sunlight and in the dark room- Rectangular shutter.

The data transmission in sunlight resulted in discovering new insights to improve the system design for outdoor setting. The received signal plot of the video shutter shown in Figure 6.13 has the signal amplitude decreasing with varying light intensity. The demodulation algorithm designed in 6.1 has a fixed threshold for the entire signal duration. To decode such a dynamic signal, adaptive threshold detection should be implemented for robust signal decoding. There is high signal interference and DC offset at short distances. This can be reduced by making hardware modifications to filter these signals. The work done in this thesis sets benchmarks for the physical layer of the sunlight based communication platform through extensive analysis in a controlled environment. This work needs to be extended further by analyzing the system in sunlight and improving its performance.

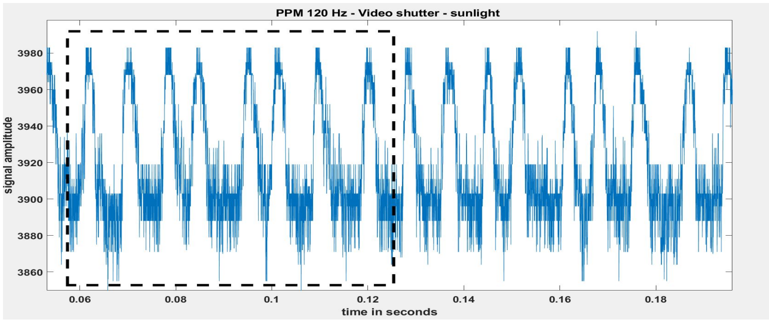

(a) Video shutter - in sunlight

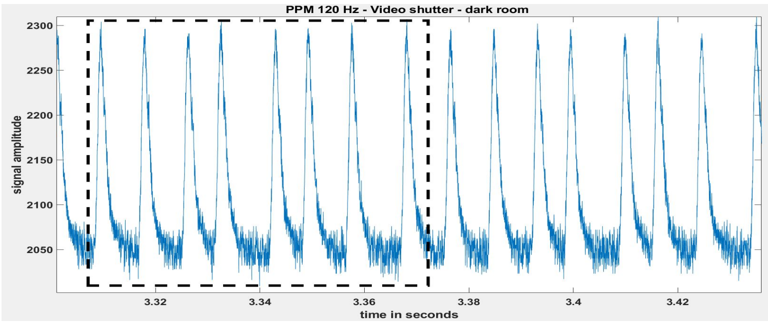

(b) Video shutter - in dark room

Figure 6.15: PPM signal transmission at 120 Hz in sunlight and in the dark room- Video shutter.

Chapter 7

Conclusion and future work

7.1 Conclusion

The work done in this thesis has led to the design of the physical layer of the sunlight based communication system. The passive communication channel proposed for mobile objects is extended to static objects. LC shutters are used as a transmission medium to modulate ambient light and transmit data.

Three commercial, off-shelf LC shutters were tested for their capability to work as a transmitter. Response time analysis was performed on the shutters and the maximum switching frequencies were computed. The voltage versus frequency behavior of the shutter was studied to validate the response time and the maximum operating frequency. The behavior of the rectangular and video shutter deemed to be suitable for use as a transmitter.

This behavior created uncertainty in choosing a suitable modulation scheme. The main objective was to transmit data such that, flickering is not visible. Modulation schemes suited for VLC with artificial light sources were tested and PPM was chosen. This modulation scheme helped to eliminate the adverse health effects caused by flickering.

Conventional decoding algorithms could not be implemented directly on this communication system. A custom offline decoding algorithm was designed to process the captured signals. The performance parameters of the shutters were measured in a controlled environment to set benchmarks for this communication platform. The power consumption per unit area is 46 mW/m^2 (213 mW/m^2) for the rectangular (video) shutter, making it an energy efficient communication alternative . The rectangular and video shutters exhibit flicker free transmission from 120 Hz and have maximum data rates of 140 bps (rectangular) and 290 bps (video) respectively. The maximum communication range for 120 Hz transmission by the small size LC shutters are 0.45 m and 1.05 m respectively. The data transmission was done in an outdoor environment with sunlight. The received signal was analyzed and the areas of improvement for robustness in the system was understood.

7.2 Future work

The research done in this thesis has resulted in a functional physical layer for the sunlight based communication system. However, there is still scope for development, especially when testing in a noisy outdoor environment. The areas of improvement in this system design are as follows:

- **Material testing and data rate improvement**

  The transmitter is currently designed using off-shelf slow switching LC shutters. This design can further improved by testing other materials for their suitability as a transmitter. Pi-cells and ferromagnetic nematic cells, photochromatic materials, active 3D glasses are other fast switching alternatives to LC shutters, which could be analyzed to work as a transmitter. The data rate can be improved by replacing the shutter with a fast switching alternative from the above options. The other option is to implement modulation schemes which can encode multiple message bits in a single pulse such as PAM [21]. A single LC shutter cannot implement this. Thus, we can use multiple LC shutters and adjust the exposure area of all the shutters to generate signals of varying amplitudes.

- **Solar power supply**

  The transmitter and receiver currently draw energy from the power source and batteries and is not an eco-friendly approach. Since sunlight is already being used for data transmission, we can harness this energy by installing solar panels on the transmitter and receiver.

- **Improve communication range**

  The communication range is highly dependent on the material dimensions, modulating frequency, light intensity and the receiver characteristics. The controllable parameter in this case is the receiver opening size which can be decreased to have a better communication range. However, this is not the best alternative in low lighting conditions and can be modified by adding a lens inside the receiver to concentrate more light as presented in [6]. A follow up project on [6] was done in parallel by Rens during my thesis period, which improved the receiver characteristics.

- **Real time decoding**

  The current decoding algorithm works offline and does post-processing on the received signals. Communication systems need to function in real time. Thus, the algorithm needs to be modified to process the signals and decode information. The signal amplitudes are consistent when tested in a dark room but are bound to vary with the light intensity in an outdoor environment. This makes it unsuitable to have a constant threshold throughout the transmission. The algorithm needs to have an adaptive threshold design to enable accurate decoding.

- **Noise reduction in outdoor lighting**

  The experiments in the thesis are done using a DC light source that replicates sunlight. The noise levels are minimal as the experiments are conducted in a dark room with a controlled environment. However, we observe that the received data in outdoor environment is accompanied with more noise due to the artificial lighting in the surroundings. Additional filters can be implemented to eliminate these unwanted frequencies. Also, the received signal gets saturated when the light intensity is very high. Modifications other than varying the receiver opening can be implemented to solve this saturation problem. An easy solution would be to install a polarizer at the receiver to limit the captured light intensity.

Bibliography

[1] Circular and video shutter. http://www.liquidcrystaltechnologies.com/Tech_Support/OAS_Cell.htm.

[2] Large liquid crystal light valve. https://www.adafruit.com/product/3330.

[3] Liquids and intermolecular forces. http://schoolbag.info/chemistry/central/105.html.

[4] Ieee recommended practices for modulating current in high-brightness leds for mitigating health risks to viewers. *IEEE Std 1789-2015*, pages 1–80, June 2015.

[5] AxiomaticNexus. Linear polarized 3d glasses and the physical shape of light waves. Physics Stack Exchange. https://physics.stackexchange.com/q/231962 (version: 2016-01-26).

[6] Rens Bloom. Channel analysis for passive communication with ambient light. MSc thesis, Delft University of Technology, The Netherlands, 2017.

[7] Christopher Schweitzer. A.g. bell speech riding on light, 2016. https://hearinghealthmatters.org/waynesworld/2016/a-g- bell-an-analog-man-inventing-speech-riding-on-light-part-2/.

[8] C. Danakis, M. Afgani, G. Povey, I. Underwood, and H. Haas. Using a cmos camera sensor for visible light communication. In *2012 IEEE Globecom Workshops*, pages 1244–1248, Dec 2012.

[9] K. Jerome, V. Tony, R. Vinayak, and K. J. Dhanaraj. Indoor navigation using visible light communication. In *2014 Texas Instruments India Educators' Conference (TIIEC)*, pages 46–52, April 2014.

[10] D. Caicedo K. Warmerdam, A. Pandharipande and M. Zuniga. Visible light communications for sensing and lighting control. volume 16, pages 6718–6726. IEEE, September 2016.

[11] Lachezar Komitov and Gurumurthy Hegde. Fast switching liquid crystal display modes. 8280, 02 2012.

[12] Kullabs. Electromagnetic spectrum. https://www.kullabs.com/classes/subjects/units/lessons/notes/note-detail/1823.

[13] Ye-Sheng Kuo, Pat Pannuto, Ko-Jen Hsiao, and Prabal Dutta. Luxapose: Indoor positioning with mobile phones and visible light. In *Proceedings of the 20th Annual International Conference on Mobile Computing and Networking*, MobiCom '14, pages 447–458, New York, NY, USA, 2014. ACM.

[14] Jiangtao Li, Angli Liu, Guobin Shen, Liqun Li, Chao Sun, and Feng Zhao. Retro-vlc: Enabling battery-free duplex visible light communication for mobile and iot applications. In *Proceedings of the 16th International Workshop on Mobile Computing Systems and Applications*, HotMobile '15, pages 21–26, New York, NY, USA, 2015. ACM.

[15] Mark Kuckian Cowan. Liquid crystal displays: An overview. http://www.battlesnake.co.uk/_uni/lcd.htm.
[16] Mary McMahon. What is a heliograph? https://www.wisegeek.com/what-is-a-heliograph.htm.
[17] M. Nakajima and S. Haruyama. Indoor navigation system for visually impaired people using visible light communication and compensated geomagnetic sensing. In *2012 1st IEEE International Conference on Communications in China (ICCC)*, pages 524–529, Aug 2012.
[18] A. Pradana, N. Ahmadi, T. Adiono, W. A. Cahyadi, and Y. Chung. Vlc physical layer design based on pulse position modulation (ppm) for stable illumination. In *2015 International Symposium on Intelligent Signal Processing and Communication Systems (ISPACS)*, pages 368–373, Nov 2015.
[19] S. Rajagopal, R. D. Roberts, and S. Lim. Ieee 802.15.7 visible light communication: modulation schemes and dimming support. *IEEE Communications Magazine*, 50(3):72–82, March 2012.
[20] Temkar Ruckmongathan, Prabhjot Juneja, and A R Shashidhara. A simple technique for measurement of the voltage dependent capacitance of pixels in liquid crystal displays. 10 2006.
[21] S. Shao, A. Khreishah, and H. Elgala. Pixelated vlc-backscattering for self-charging indoor iot devices. *IEEE Photonics Technology Letters*, 29(2):177–180, Jan 2017.
[22] M. Siekkinen, M. Hiienkari, J. K. Nurminen, and J. Nieminen. How low energy is bluetooth low energy? comparative measurements with zigbee/802.15.4. In *2012 IEEE Wireless Communications and Networking Conference Workshops (WCNCW)*, pages 232–237, April 2012.
[23] Qing Wang, Marco Zuniga, and Domenico Giustiniano. Passive communication with ambient light. In *Proceedings of the 12th International on Conference on Emerging Networking Experiments and Technologies*, CoNEXT '16, pages 97–104, New York, NY, USA, 2016. ACM.
[24] Makoto Watanabe, Keiichiro Ishihara, Takeyuki Tsuruma, Yasuhiko Iguchi, Yoshiharu Nakajima, and Yasuhito Maki. Macro-modeling of liquid crystal cell with veriloga. In *2007 IEEE International Behavioral Modeling and Simulation Workshop*, pages 132–137, Sept 2007.
[25] Wikipedia. Electromagnetic spectrum — Wikipedia, the free encyclopedia.
[26] Wikipedia. Heliograph — Wikipedia, the free encyclopedia.
[27] Wikipedia. Photophone — Wikipedia, the free encyclopedia.
[28] Wikipedia. Radio spectrum — Wikipedia, the free encyclopedia.
[29] Xieyang Xu, Yang Shen, Junrui Yang, Chenren Xu, Guobin Shen, Guojun Chen, and Yunzhe Ni. Passivevlc: Enabling practical visible light backscatter communication for battery-free iot applications. In *Proceedings of the 23rd Annual International Conference on Mobile Computing and Networking*, MobiCom '17, pages 180–192, New York, NY, USA, 2017. ACM.
[30] Zhice Yang, Zeyu Wang, Jiansong Zhang, Chenyu Huang, and Qian Zhang. Wearables can afford: Light-weight indoor positioning with visible light. In *Proceedings of the 13th Annual International Conference on Mobile Systems, Applications, and Services*, MobiSys '15, pages 317–330. ACM, 2015.